June 2023

Stable Isotope Analysis of Doryteuthis (Amerigo) pealeii Eye Lenses to Determine Migratory Patterns in the Eastern Gulf of Mexico Using Statoliths for Age Determination

Hannah M. Schwaiger
University of South Florida

Stable Isotope Analysis of *Doryteuthis (Amerigo) pealeii* Eye Lenses to Determine Migratory Patterns in the Eastern Gulf of Mexico Using Statoliths for Age Determination

by

Hannah M. Schwaiger

A thesis submitted in partial fulfillment
of the requirements for the degree of
Master of Science
College of Marine Science
University of South Florida

Co-Major Professor: Heather Judkins, Ph.D.
Co-Major Professor: Ernst Peebles, Ph.D.
Lisa Hendrickson, MS, Northeast Fisheries Science Center, NOAA

Date of Approval:
May 30, 2023

Keywords: isoscape, longfin inshore squid, life history, statolith, West Florida Shelf, Loliginidae

ACKNOWLEDGMENTS

I would like to thank my committee as a whole for always being supportive, patient, and willing to hash out any ideas and questions that came up during this research. I would especially like to thank my major professor, Dr. Heather Judkins, for providing me with infinite guidance and always being encouraging. I would also like to thank Dr. Ernst Peebles, my co-advisor, for always being welcoming and willing to sit down with me for as long as it took to help me when I needed guidance. I would also like to thank my committee member Lisa Hendrickson for providing new perspectives and insight into species- and fisheries-specific details. Additionally, I would like to thank everyone with Florida Fish and Wildlife Conservation Commission (FWC) and Southeast Area Monitoring and Assessment Program (SEAMAP) for providing all of the specimens and catch data used in this study, and especially Janessa Fletcher for her guidance with compiling data. I would also like to thank Ethan Goddard for his assistance with stable isotope analysis. I would also like to thank Brenna Meath for providing the data on *D. plei* and dissecting specimens from 2015, as well as Sami Francis and Dr. David Naar at the College of Marine Science for their guidance along this journey.

I am extremely grateful to my lab mates in both the Judkins and Peebles labs for not only helping me when I hit a roadblock, but also being an amazing support system for me. Thank you to all of my friends for always being encouraging and reminding me how important it is to take breaks. Last but not least, thank you so much to my parents, my brother Jordan, and my partner,

Ben, for all the late-night pep talks and love that saw me through this degree. Thank you all for helping me make my dreams come true.

TABLE OF CONTENTS

List of Tables iii

List of Figures iv

Abstract v

I. Introduction 1

I.I Determination of Age Using Statoliths 5
I.II Stable isotope analysis of eye-lenses to track migration patterns 7
I.III Figures 10

II. Methods 12

II.I Collection and Dissection 12
II.II Age determination from statolith increment counts 13
II.III Stable isotope analysis of eye-lens laminae 15
II.IV Migration pattern comparison between *D. pealeii* and *D. plei* in the GoM 16
II.V Tables and Figures 17

III. Results 23

III.I Statolith analyses 23
III.II Stable isotope analyses 24
III.III Migration patterns related to life history 29
III.IV Migration patterns of *D. pealeii* and *D. plei* 30
III.V Tables and Figures 32

IV. Discussion 40

IV.I Ages of GoM *D. pealeii* 40
IV.II Migration patterns of *D. pealeii* and Life History Correlations 41
IV.III Migration patterns of *D. pealeii* and *D. plei* 45
IV.IV Future Research 46

Works cited 47

Appendices 53

Appendix A. Linear regressions of $\delta^{13}C$ vs. diametric lamina midpoint for all specimens 54
Appendix B. Linear regressions of $\delta^{15}N$ vs. diametric lamina midpoint for all specimens 55
Appendix C. Spearman's rank correlations of $\delta^{15}N$ vs. $\delta^{13}C$ for all specimens.....56

LIST OF TABLES

Table 1. Specimen summary table 17

Table 2. $\delta^{13}C$ and diametric eye-lens lamina midpoint isotope regression trends 32

Table 3. $\delta^{15}N$ and diametric eye-lens lamina midpoint isotope regression trends 33

Table 4. $\delta^{13}C$ vs. $\delta^{15}N$ isotope regression trends using Spearman's correlation 34

LIST OF FIGURES

Figure 1. Map of *Doryteuthis pealeii* collections via SEAMAP bottom-trawl surveys on the West Florida Shelf, including specimen ID code and NMFS zones (numbered polygons; 3 is south, 4 is southern middle, 5 is northern middle, 6 is north) for 2015 and 2019 10

Figure 2. Distribution heat map of *Doryteuthis pealeii* collection via biannual SEAMAP bottom-trawls surveys along the West Florida Shelf, in June (top) and October (bottom) from 2014-2021. Top: June SEAMAP cruises 2014-2021; Bottom: October SEAMAP cruises 2014-2021 11

Figure 3. Specimen hatch month frequency histogram 20

Figure 4. Specimen age distribution frequency histogram 21

Figure 5. Age precision analysis 22

Figure 6. Boxplots of age (days), mantle length (mm), weight (g), and eye-lens diameter (mm) per zone 36

Figure 7. Migration pattern tallies according to stable isotope trends 37

Figure 8. Scatterplots of $\delta^{13}C$ and $\delta^{15}N$ values with eye-lens laminar midpoint for all specimens 38

Figure 9. $\delta^{13}C$ vs. $\delta^{15}N$ eye-lens core values 39

ABSTRACT

Doryteuthis (Amerigo) pealeii is a common fisheries squid that occurs in the Gulf of Mexico (GoM) and along the east coast of the United States. These squid are an important link in the food web, linking higher and lower trophic positions (Madsen et al., 2007), and they are also used for human consumption. The migration patterns of *D. pealeii* populations in the northwestern North Atlantic have been thoroughly studied when compared to those in the GoM. This research aims to combine statolith aging and stable isotope analysis to enhance the understanding of *D. pealeii* migration patterns throughout their short, sub-annual lifespan along the West Florida Shelf in the GoM. Individual specimens were aged via statoliths, and $\delta^{13}C$ and $\delta^{15}N$ stable isotopes were analyzed within individual eye-lens laminae of *D. pealeii* specimens. These were compared to known isoscapes present along the West Florida Shelf to determine overall migration patterns, which were then compared to variables such as specimen age and hatch month to document any potential relationships. Among individual squid, the most common migration patterns observed in this study were northeastward (35%) and eastward (32%) movement. When compared with hatch month, this suggests the *D. pealeii* in the GoM exhibit similar migration patterns to those off the northeastern coast of the United States – hatching and spending the colder months offshore, then moving inshore during spring and early summer. This study suggests that maternal contribution of isotope ratios is present in the eye-lens cores of specimens, which allows us to make inferences about the spawning grounds from which the specimens included in this study hatched. Core $\delta^{13}C$ and $\delta^{15}N$ ratios suggest individuals from the

most northern National Marine Fisheries Service (NMFS) statistical zone included in this study remain in the same area they were spawned in, while the other NMFS zones included here intermix. The migration patterns of *D. pealeii* were compared to those of *D. plei* observed by Meath et al. (2019) to determine any potential overlap in migration patterns between the two species. Over half of those examined for both species exhibited isotope trends that suggested either northeastward or eastward movement over the course of their lives. This research will contribute to the understanding of the migration patterns of the *D. pealeii* population within the GoM, allowing fishery management to better regulate populations, maximize harvest, and prevent future overfishing in this area.

I. INTRODUCTION

Doryteuthis (Amerigo) pealeii was originally described as *Loligo pealei* in 1821 (Lesueur, 1821) and is commonly known as the longfin inshore squid. It is distributed throughout the western Atlantic Ocean from Newfoundland to the Gulf of Venezuela, including the Gulf of Mexico (GoM), and is a member of the family Loliginidae (LaRoe, 1967; Cadrin, 1998; Vecchione et al., 2005; Bullard, 2012). Loliginid squids are a targeted marine fishery along the eastern coast of the United States, commonly found from the Gulf of Maine to the GoM (Voss, 1956; Serchuk & Rathjen, 1974). In the United States, *D. pealeii* populations are primarily fished and monitored along the Atlantic coast between Cape Hatteras, North Carolina, and Georges Bank, but they are also caught in the northern GoM (Serchuk & Rathjen, 1974; Cadrin, 1998; Buresch et al., 2006; Jereb & Roper, 2010; Arkhipkin et al., 2015).

The *D. Pealeii* population in the GoM is genetically distinct from the *D. pealeii* population in the Northwest Atlantic Ocean (hereafter referred to as the "northeast population") (Herke & Foltz, 2002; Buresch et al., 2006; Shaw et al., 2010). Herke and Foltz (2002) suggests that strong currents in the Straits of Florida do not allow the passage of either paralarvae or adult *D. pealeii* between the two populations, preventing genetic mixing. This creates a natural boundary between the two *D. pealeii* stocks in the U.S. (GoM and northeast population), allowing us to conduct separate stock assessments on them in order to manage both stocks effectively.

The northeastern population of *D. pealeii* is found north of Cape Hatteras, North Carolina, and is known to migrate inshore to shallower waters during the warmer months (March-October), and then offshore into deeper waters near the edge of the continental shelf and upper slope during late fall to overwinter (eggs and larvae typically found inshore spring to fall) (Cadrin, 1998; Macy & Brodziak, 2001; Jacobson, 2005; Jereb & Roper, 2010). This species inhabits depths between the surface and 400 m, typically living close to (and sometimes resting on) the bottom during the day and moving towards the surface at night (Jacobson, 2005; Jereb & Roper, 2010; Jacobson et al., 2015).

D. pealeii serves as a link in the food web between lower and higher trophic positions which must be considered when evaluating this fishery's sustainability (Jereb & Roper, 2010; Staudinger & Juanes, 2010). Finfish and elasmobranchs are common predators of juvenile and sub-adult squid, while marine mammals and the *D, pealeii* fishery both target adult squid, (Staudinger & Juanes, 2010). Overfishing of predators that feed on squid may lead to a rise in *D. pealeii* populations, consequentially decreasing the populations of juvenile fish these squid feed on (Hunsicker & Essington, 2008). The *D. pealeii* population must be monitored in an effort to prevent imbalance in the food web (Hunsicker & Essington, 2008).

Currently, the *D. pealeii* fishery in the GoM is not regulated by any of the states that comprise the Gulf States Marine Fisheries Commission (GSMFC), but landings are reported as "Loliginidae" and are very low in comparison to the *D. pealeii* landings harvested from the northeastern population. Loliginidae landings downloaded from the GSMFC Fisheries Information Network (FIN) database (GSMFC, 2023) report the average total landings of all GoM states combined (in metric tons) during a period when all states had landings greater than zero, and mention the states that comprised a majority of the total landings during the same time

period (states can only regulate waters shoreward of three nautical miles). Occasional trips have been conducted in Florida that appeared to be targeting squid, but the vast majority of landings reported are likely from bycatch. No other state indicated any targeted trips for squid (Gregg Bray, GSMFC, GulfFIN Program Coordinator, pers. comm., March 15, 2023). No loliginid squid are currently subject to a federal Fishery Management Plan in the GoM (L. Hendrickson, NOAA, Northeast Fisheries Science Center, pers. comm., March 19, 2023).

The migration patterns of *D. pealeii* in the GoM are currently not well known due to challenges in distinguishing among *D. pealeii*, *Doryteuthis (Doryteuthis) plei* (Blainville, 1823) and *Doryteuthis (Doryteuthis) roperi* (Cohen, 1976) at sea during research surveys, where identification is often based solely on external morphology (Cohen, 1976; Vecchione, 1988; K. E. Carpenter, 2002; Jereb & Roper, 2010; Arkhipkin et al., 2015). While at sea in the GoM, misidentifications among these three species are common due to overlapping habitat and similar morphology (Cohen, 1976; Hixon et al., 1980; Vecchione, 1988; K. E. Carpenter, 2002; Vecchione et al., 2005; Jereb & Roper, 2010). This is not a concern off the northeastern coast of the United States because the northern limit for *D. plei* distribution is Cape Hatteras, North Carolina, which is the southern limit for the *D. pealeii* fishery off the northeastern U.S. coast (Jereb & Roper, 2010). Both *D. pealeii* and *D. plei* (not *D. roperi*) have suckers on their ventral buccal lappets, and both species' tentacular clubs have over 26 transverse rows of suckers, while *D. roperi* has fewer than 25 (K. E. Carpenter, 2002). Some morphological characteristics used to identify between *D. pealeii* and *D. plei* are size-dependent, such as the ratio of fin length to mantle length (only for *D. pealeii* mantle lengths over 55 mm or *D. plei* mantle lengths less than 95 mm) (K. E. Carpenter, 2002). The most common character used for identification between *D. pealeii* and *D. plei* is the ratio of the greatest width of the vane of the gladius to the greatest

width of the free rachis (ratio of 1.5 to 2.4 for *D. plei*, 2.4 to 3.7 for *D. pealeii*), which was used to confirm identifications in this study (Cohen, 1976; K. E. Carpenter, 2002). This small difference is difficult to observe at sea, which can lead to inaccurate identifications in the GoM. Further research on their migration patterns throughout their life history could greatly benefit potential future management of the *D. pealeii* population in the GoM, as well as aid in identification between loliginids in the GoM.

Environmental factors such as temperature play a major role in determining the rate at which individuals mature, spawn, and develop (Forsythe, 2004; Jacobson, 2005; Jereb & Roper, 2010). *Doryteuthis pealeii* growth rates increase significantly when water temperature increases by 5°C (Hatfield et al., 2001; Forsythe, 2004). The water temperature in the northern GoM is typically 24°C or warmer in the spring (Love et al., 2013), and the northeastern *D. pealeii* population is known to be found in temperatures between 8-26°C throughout its lifespan (Jacobson, 2005). During the winter, temperatures between these locations are more similar to one another (Locarnini et al., 2019).

The Florida Fish and Wildlife Conservation Commission (FWC) conducts research bottom-trawl surveys (summer shrimp and fall groundfish) twice a year in June and October along the West Florida Shelf as part of the Southeast Area Monitoring and Assessment Program (SEAMAP) (Figure 1, 2) ("SEAMAP Operations Manual for Trawl and Plankton Surveys," 2019). SEAMAP has been a cooperative since 1982, with the goal of collecting and compiling fishery-independent data primarily for fishery stock assessments and management. As part of the SEAMAP survey protocol, the *D. pealeii* population is sampled along with *D. plei* and *D. roperi*. However, as previously mentioned, identification at sea to species level is not always possible in the GoM due to the similar gross morphologies among these three species (Cohen, 1976;

Vecchione, 1988; K. E. Carpenter, 2002; Jereb & Roper, 2010; Arkhipkin et al., 2015), and therefore a subsample of individuals is collected to verify species identification post-cruise in the lab. Density heat maps of *D. pealeii* catch data from Spring (June) and Fall (October) SEAMAP cruises conducted on the West Florida Shelf between 2014 and 2021 have been included for reference (Figure 2). Heat maps were based on species identifications from each SEAMAP cruise by museum staff of the Florida Biodiversity Collection at FWRI, from 2014 to 2021. For statistical purposes, when species-level identification was not available, one third of confirmed *Doryteuthis spp.* were considered to be *D. pealeii* (Janessa Fletcher, FWRI, SEAMAP Collection Manager, pers. comm., September 15, 2022). SEAMAP cruises sample randomly within each National Oceanic and Atmospheric Administration (NOAA) National Marine Fisheries Service (NMFS) statistical zone for each cruise, sampling a variety of depths within each zone (choosing from within two depth ranges, proportional to the available sampling surface area within each zone after removing areas that are unable to be sampled), which removes sampling bias from the *D. pealeii* distribution map included in this study (Figure 2) ("SEAMAP Operations Manual for Trawl and Plankton Surveys," 2019). Figure 2 is representative of the distribution of *D. pealeii* along the West Florida Shelf between 2014 and 2021.

I.I Determination of Age Using Statoliths

Most of a squid's body is soft tissue and undergoes metabolic turnover relatively quickly. There are a few hard, archival structures that can be used as biological tracers for determining factors such as age and migration trends throughout an individual's lifetime. These archival tissues and structures include the eye-lenses (Hunsicker et al., 2010), statoliths (Arkhipkin, 2005;

Ceriola & Milone, 2007; Liu et al., 2015), beak (Liu et al., 2015), and gladius (Perez et al., 1996).

Squid eye-lenses (Parry, 2003), like fish eye-lenses (Wallace et al., 2014), and statoliths (Macy, 1995) form periodic layers and growth increments, respectively, as a result of growth (Jackson, 1994; Macy, 1995; Brodziak & Macy, 1996; Macy & Brodziak, 2001; Parry, 2003; Ceriola & Milone, 2007; Hunsicker et al., 2010; Wallace et al., 2014; Meath, 2017). The time required for each layer of eye-lens to form in *D. pealeii* is currently unknown, but their statoliths show daily growth increments (Macy, 1995; Brodziak & Macy, 1996). Both squid beaks (Clarke, 1965; Liu et al., 2015) and gladii (Bizikov, 1991) have also been used to age squid in previous studies (Clarke, 1965; Bizikov, 1991).

Statoliths are small, hard calcareous structures located within the paired statocysts (one in each), which assist with overall spatial orientation and balance in the water column (Jackson, 1994; Hatfield et al., 2001; Jereb & Roper, 2010). Statoliths are composed of calcium carbonate (specifically the mineral aragonite), which forms concentric layers around a central natal ring; statolith morphology can be species-specific (Radtke, 1983; Lipinski et al., 1998; Ceriola & Milone, 2007). The analysis of growth increments in these structures has been used in multiple studies to determine the age of various cephalopod species (Rosenberg et al., 1981; Radtke, 1983; Brodziak & Macy, 1996; Dawe & Beck, 1997; Lipinski et al., 1998; Hatfield et al., 2001; Macy & Brodziak, 2001; Forsythe, 2004; Ceriola & Milone, 2007; Arkhipkin & Shcherbich, 2012). For many squid species, including *D. pealeii* (Macy, 1995), it is assumed that growth rings are formed daily (Jackson, 1994; Brodziak & Macy, 1996; Lipinski et al., 1998; Macy & Brodziak, 2001; Ceriola & Milone, 2007). As a result, statolith-based age determination is the

most often used method for age identification of *D. pealeii* (Macy, 1995; Brodziak & Macy, 1996).

The growth increments in *D. pealeii* (Macy, 1995) statoliths have been used to age this species in multiple studies (Jackson, 1994; Brodziak & Macy, 1996; Macy & Brodziak, 2001). Studies focusing on the northeastern *D. pealeii* population (collected from both commercial fishing and research surveys, study dependent) have suggested a lifespan of less than one year, with year-round spawning that peaks according to season and geographic region (Macy, 1995; Brodziak & Macy, 1996; Hatfield et al., 2001; Macy & Brodziak, 2001; Hatfield & Cadrin, 2002; Jacobson, 2005; Jereb & Roper, 2010). The northeastern population of *D. pealeii* spawns in two intra-annual cohorts (Macy & Brodziak, 2001).

In order to properly analyze the statolith, it must be properly mounted, ground down, polished, and viewed under a transmitted-light microscope to minimize increment enumeration error, and some studies use semi-automated techniques for aging (Brodziak & Macy, 1996; Lipinski et al., 1998; Ceriola & Milone, 2007). Statolith analysis in this study focused on age from hatching, which is marked by the natal ring in *D. pealeii* (Macy, 1995).

I.II Stable isotope analysis of eye-lenses to track migration patterns

Radabaugh et al. (2013) used stable isotope data obtained from fish tissue, benthic algae (via sea-urchin stomachs), and filtered particulate organic matter (POM, which largely consisted of phytoplankton) samples to describe $\delta^{13}C$ and $\delta^{15}N$ isoscapes on the West Florida Shelf, which covers the entire sampling area for the present study (Radabaugh et al., 2013). An isoscape, or isotopic map, refers to how the stable isotope ratios of $\delta^{13}C$ and $\delta^{15}N$ in environmental materials

and organisms vary with geographic distribution (Bowen, 2010; Radabaugh et al., 2013). The $\delta^{15}N$ isoscape in the GoM has been determined to be relatively stable, often reflecting the presence of eutrophic, mesotrophic, or oligotrophic waters, and is likely being influenced by runoff and river input over time (e.g. the Mississippi and other rivers to the northwest), as well as nitrogen fixation that is more prevalent in more southerly, oligotrophic waters (Radabaugh et al., 2013; Radabaugh & Peebles, 2014). The mass balance of nitrogen inputs from land leads to empirically observed higher $\delta^{15}N$ in the north-central GoM, whereas nitrogen fixation leads to lower $\delta^{15}N$ in the southeastern (more oligotrophic) region of the GoM (E. J. Carpenter et al., 1997; Montoya et al., 2002; Montoya, 2007; Radabaugh et al., 2013; Radabaugh & Peebles, 2014; Sharp, 2017). The $\delta^{13}C$ isoscape in the GoM is influenced by the dominant basal resources (primary-producer types) and their population growth rates (fast growth tends to inhibit fractionation), as these basal-resource isotopes are taken up by secondary producers in the area and are passed along to higher trophic positions in the food web (Radabaugh et al., 2013; Radabaugh & Peebles, 2014).

Stable isotopes have previously been used to assess trophic positions and migration patterns of multiple marine species in the GoM (Fry, 1981; Hobson, 1999; Wallace et al., 2014; Michaud, 2022). In cephalopods, stable isotope analysis of eye-lenses has been used to investigate dietary information and trophic position, as well as make inferences about lifelong geographic movement and natal origins (Onthank, 2013; Liu et al., 2020). For squid, eye-lenses can be used in stable isotope analysis to gain information about migration patterns and trophic position, as previously used in *D. plei* by Meath (2017) (Radabaugh et al., 2013; Radabaugh & Peebles, 2014; Wallace et al., 2014). As *D. plei* grows, crystallin proteins are added to the exterior surface of the eye-lens, synthesizing layers (laminae) such that the oldest part of the eye-

lens is located at the center and the youngest part of the eye-lens is the exterior lamina (Meath, 2017). In *D. pealeii*, the youngest part of the eye-lens is formed prior to hatching (Arnold, 1966). The proteins in each eye-lens lamina can be analyzed to determine $\delta^{13}C$ and $\delta^{15}N$ isotopic ratios present in the specimen's body when each specific lamina was formed, which can then be compared to isoscapes previously determined for the eastern GoM (Radabaugh et al., 2013; Radabaugh & Peebles, 2014). This is possible because the $\delta^{13}C$ and $\delta^{15}N$ isotopes present in animals originate from their food sources, which can be traced back to the basal primary producers (DeNiro & Epstein, 1978; Peterson & Fry, 1987).

Basal-resources (primary-producers such as phytoplankton, benthic microalgae, benthic macroalgae, etc.) receive their initial isotopic ratios from their surrounding environments, but in the case of $\delta^{13}C$ may modify (fractionate) these ratios in characteristic manners, depending on basal-resource type. In comparison, $\delta^{15}N$ ratios in marine primary producers are relatively conservative, primarily reflecting the isotopic characteristics of different nutrient sources (decomposed animal waste, fixed atmospheric nitrogen, anthropogenic fertilizer, etc.). Isotopic fractionation within the food web (trophic fractionation) causes $\delta^{13}C$ and $\delta^{15}N$ ratios to increase with every increase in trophic position (Fry, 1981; Peterson & Fry, 1987; Hobson, 1999; McCutchan Jr et al., 2003). Comparative analysis of these ratios can be used to determine the general change in trophic and geographic position ("ecogeography") as new eye-lens layers are formed, revealing the general habitat changes of the individual itself. Through this comparison, it is possible to determine a generalized lifelong migration pattern for *D. pealeii*.

The goal of this study was to gain knowledge about the age and migration patterns of *D. pealeii* on the West Florida Shelf using statolith and stable isotope analyses. The questions addressed were: 1) What is the age range of mature *D. pealeii* in the GoM? 2) What are the

migration patterns of *D. pealeii* specimens along the West Florida Shelf? 3) Is there any relationship between migration patterns and life history of *D. pealeii*? and, 4) How do the migration patterns of *D. pealeii* compare to those of *D. plei*?

I.III Figures

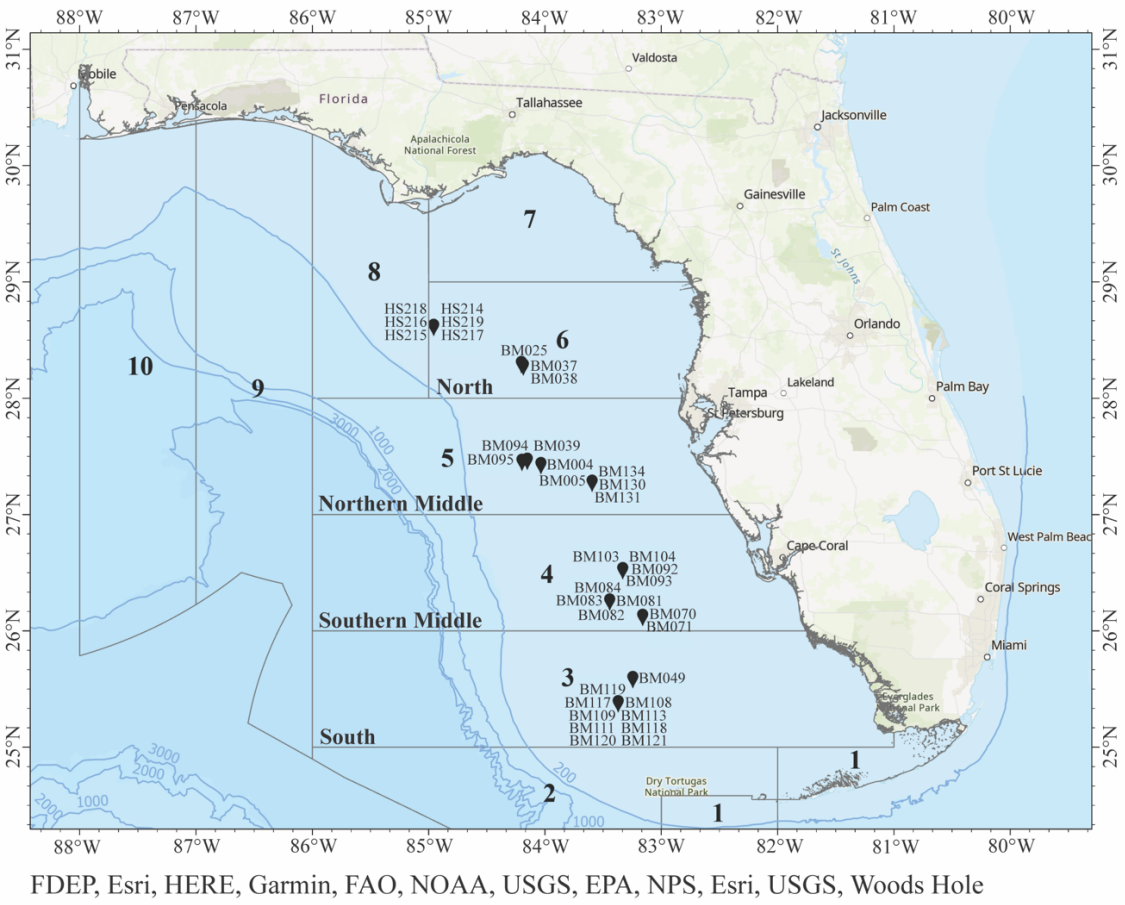

Figure 1. Map of *Doryteuthis pealeii* collections via SEAMAP bottom-trawl surveys on the West Florida Shelf, including specimen ID code and NMFS zones (numbered polygons; 3 is south, 4 is southern middle, 5 is northern middle, 6 is north) for 2015 and 2019.

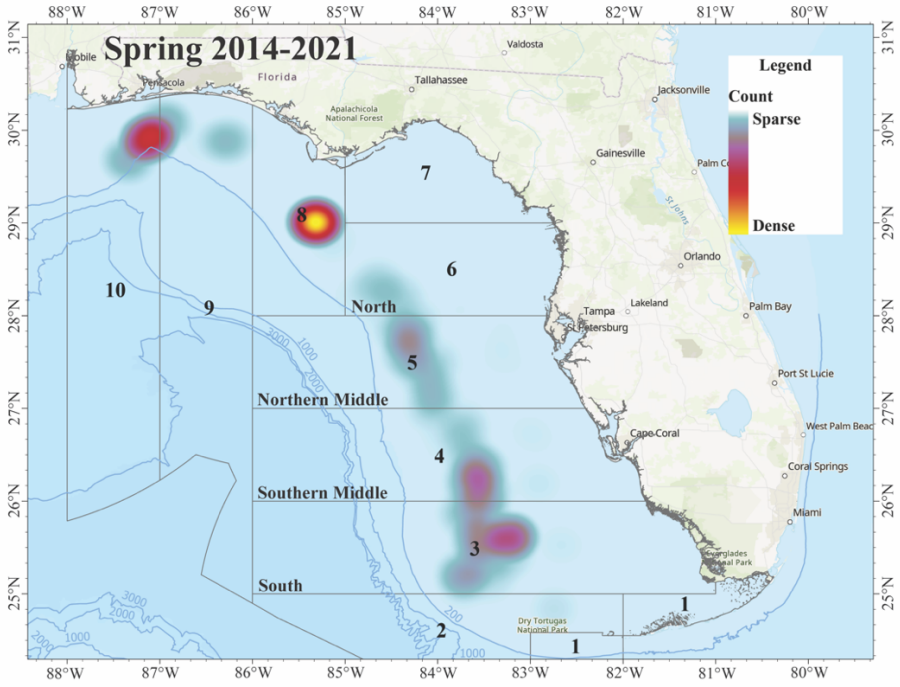

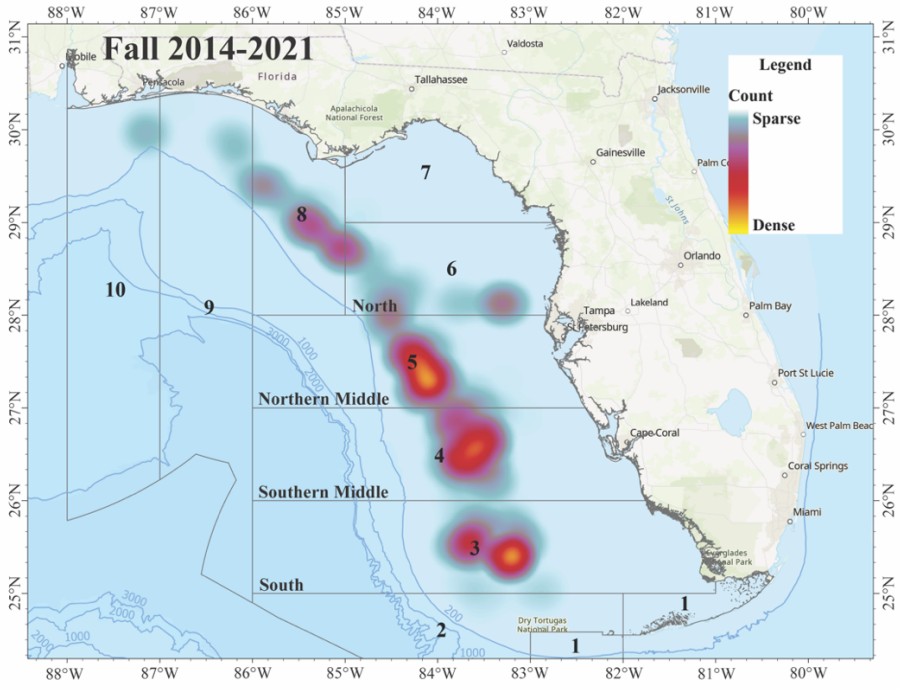

Figure 2. Distribution heat map of *Doryteuthis pealeii* collection via biannual SEAMAP bottom-trawls surveys along the West Florida Shelf, in June (top) and October (bottom) from 2014-2021. Top: June SEAMAP cruises 2014-2021; Bottom: October SEAMAP cruises 2014-2021.

II. METHODS

II.I Collection and Dissection

This study focused on the West Florida Shelf, which is only a portion of the *D. pealeii* habitat in the GoM, due to the sampling areas covered by the Fall SEAMAP cruises in 2015 and 2019. Zones included in SEAMAP surveys that did not have at least ten *D. pealeii* specimens available (zones 1,2,7, and 8) were omitted from this study. A total of 40 *D. pealeii* specimens were collected during two fall (October) SEAMAP research bottom-trawl surveys conducted on the West Florida Shelf, in the northeast GoM, by FWC. Thirty-one specimens were collected in 2015 and nine were collected in 2019 within zones 3-6 (Figure 1). The additional nine specimens from 2019 were required to increase the sample size from each zone. Five males and five females per zone were initially analyzed, but three specimens were omitted from this study due to issues during stable isotope analysis or their small size, resulting in insufficient eye-lens material to be tested during stable isotope analysis using the equipment available at the time of this study. A total of 37 specimens are included in this study from zones three through six (Figure 1, Table 1). Five males and five females from zone three, five males and five females from zone four, four males and four females from zone five, and four males and five females from zone six were included in this study. All specimens were frozen upon collection at sea.

Once specimens were thawed, identifications and sex were confirmed (K. E. Carpenter, 2002). For each specimen, sex, mantle length (mm), and weight (g) (using Ohaus Scout Pro

SP202 scale, scale division: d = 0.01 g) were documented (Table 1). Specimens from 2015 ("BM") had already been dissected, and the frozen samples provided consisted of both eye-lenses and statoliths, which were used in this study. Specimens from 2019 ("HS") were provided frozen whole, and all were thawed for processing. Like the 2015 samples, the same biological data were collected from each specimen (Table 1), along with the extraction of both statoliths. Statoliths were frozen with the rest of the sample until analysis (Kristensen, 1980; Ceriola & Milone, 2007).

II.II Age determination from statolith increment counts

Statoliths were kept frozen until analysis (Kristensen, 1980; Ceriola & Milone, 2007). Methods outlined in Ceriola and Milone (2007) were used in conjunction with Brodziak and Macy (1996) to extract, mount, and process the *D. pealeii* statoliths, as well as conduct statolith increment counts (Macy, 1995).

Statolith extraction, mounting, and processing was done under an Olympus SZ61 zoom stereo microscope. The statoliths were mounted on microscope slides using Crystal Bond™ 509 (Ceriola & Milone, 2007). After mounting, the methods described by Brodziak and Macy (1996) for *D. pealeii* were followed, stopping after both sides were ground once to make statolith reading as easy as possible while also minimizing the risk of overgrinding, which would have resulted in an unreadable statolith. Grinding both the anterior and posterior surfaces of *D. pealeii* statoliths is common practice (Macy, 1995; Brodziak & Macy, 1996), as it provides a cross-section of the statolith, making it possible to count concentric growth increments that grow in all directions outward from the natal ring. Samples were ground with Taytools aluminum oxide

lapping films in sizes 30 µm, 12 µm, 5 µm, and 3 µm (Brodziak & Macy, 1996; Ceriola & Milone, 2007), and this process was monitored using the Olympus SZ61 zoom stereo microscope throughout the grinding process. The exposed surfaces of the statoliths were not coated with resin as suggested by Brodziak and Macy (1996). This step was omitted to minimize the possible introduction of dust trapped in the resin while cooling, which could potentially interfere with statolith readings.

Statolith increment counts were completed by hand using a PAXcam digital microscope camera to stream the live feed onto a computer monitor. A rotatable polarizing light filter was used to aid in visualization of statolith increments (Brodziak & Macy, 1996). Elements of the live feed, such as the image contrast and hue, were adjusted using the PAXcam software to aid increment analysis. Increment counts were recorded starting with the natal ring. In cases where the natal ring was not obvious, an ocular micrometer was used to estimate the location of the natal ring – roughly 100-120 µm in diameter according to Brodziak and Macy (1996) – and the most prominent increment closest to this estimation was considered the natal ring. Increments located nearest the edge of each statolith were often close together and unable to be counted, requiring estimation. Areas where increments were unable to be counted, or "white areas," were estimated by measuring the white area on the computer monitor using Bel-Art H-B Instrument SP Scienceware calipers, and then using this measurement on the calipers to compare to an adjacent area that was able to be read (Ceriola & Milone, 2007). All statoliths used in this study had less than 15% of the whole statolith surface covered by white areas (González et al., 1996; Ceriola & Milone, 2007). To increase accuracy and estimate precision, the number of growth increments for each statolith were counted three times, each count on different days, and the mean of the three counts was used as the estimated age (Table 1) (Jackson, 1994; Brodziak &

Macy, 1996; Macy & Brodziak, 2001). Frequency histograms were created for hatch month (back calculated from capture date; Figure 3) and age distribution (Figure 4). In Figure 4, ages were binned into four equally sized age ranges. Precision was evaluated for the age estimates by analyzing all three individual age estimates per specimen (Figure 5).

II.III Stable isotope analysis of eye-lens laminae

Eye-lenses were extracted from each specimen, following the methodology described by Meath (2017). The right eye-lenses from all 37 specimens were selected to be used for stable isotope analysis and delaminated using the wet method of separating the lens laminae from Meath (2017). Eye-lens core sizes were kept between 1.3 and 1.0 mm in diameter, and other eye-lens lamina were kept at a minimum of 0.1 mm thick so that dried samples would provide at least 300 to 600 µg for stable isotope analysis, as in Meath (2017). After each lamina was removed, it was placed on a labeled pane of glass to dry. Diametric lamina midpoint was calculated for each eye-lens lamina by taking the average of two eye-lens diameter measurements – the eye-lens diameter before lamina removal, and the eye-lens diameter after lamina removal. Radial lamina midpoints for eye-lens cores were calculated by dividing the diameter of the core by four. Radial lamina midpoints were used for eye-lens cores because their isotope values are more likely to reflect the radial midpoint than either the center of the core or its outer edge (core isotopes are a mass balance of the entire core, not just its edge or center). Diametric lamina midpoints were used in the $\delta^{13}C$ and $\delta^{15}N$ isotope regressions (Appendix A, B) in order to best represent each lamina as a whole. Once laminae were dried, they were crushed with a clean razor blade and transferred to vials for stable isotope analysis.

The $\delta^{13}C$ and $\delta^{15}N$ isotopes were analyzed for each eye-lens lamina using a ThermoFinnigan Delta+XL Isotope Ratio Mass Spectrometer (IRMS), following the same protocol described in Wallace et al. (2014) and Meath (2017) used for the stable isotope analysis (Wallace et al., 2014; Meath, 2017).

Nitrogen and carbon isotopes and bulk compositions were measured by Continuous Flow Elemental Analyzer Isotope Ratio Mass Spectrometry (CF-EA-IRMS) at the University of South Florida College of Marine Science Marine Environmental Chemistry Laboratory using commonly accepted procedures (Werner et al., 1999). Isotope compositions were measured on a ThermoFinnigan Delta+XL IRMS, are reported in per mil (‰) notation and are scaled to VPDB ($d^{13}C$) and AT-Air ($d^{15}N$). Secondary reference materials (NIST 8574 $d^{13}C$ = +37.63 ± 0.10 ‰, $d^{15}N$ = +47.57 ± 0.22 ‰, N = 9.52%, C = 40.81%, C:N (molar) = 5.0; NIST 8573 $d^{13}C$ = -26.39 ± 0.09‰, $d^{15}N$ = -4.52 ± 0.12‰ N = 9.52%, C = 40.81%, C:N (molar) = 5.0) were used to normalize original measurements to the VPDB ($d^{13}C$) and AT-Air ($d^{15}N$) scales (Werner & Brand, 2001; Qi et al., 2003; Coplen et al., 2006) and to calibrate elemental N, C and C:N. Measurement uncertainties, expressed as ±1 standard deviation of n=90 measurements of a laboratory reference material (NIST1577b $d^{13}C$ = -21.69 ± 0.14‰, $d^{15}N$ = 7.83 ± 0.16‰, %N = 9.95 ± 0.48%, %C =48.04 ± 0.71%, C:N (molar) = 5.63 ± 0.27) were ±0.20 ‰ for $d^{13}C$ ±0.21 ‰ for d15N, ±4.32 %RSD for %N, ±3.03 %RSD for %C, and ±3.24 %RSD for C:N.

II.IV Migration pattern comparison between *D. pealeii* and *D. plei* in the GoM

In the GoM, *D. pealeii* and *D. plei* can be difficult to distinguish at sea, and are often collected together. The inferred individual-specific migration patterns of *D. pealeii* were

compared to those of *D. plei* as determined by Meath et al. (2019), which included 42 individuals (21 males, 21 females). The sample location of this study was kept within the same area of the West Florida Shelf as that of Meath (2017). However, the geographic distribution of *D. pealeii* specimens was smaller. The statistical analysis methods for the stable isotope data were kept similar to Meath (2017) in order to facilitate adequate comparison between the two studies.

II.V Tables and Figures

Table 1. Specimen summary table. Includes NMFS zone, station, region, collection year, sex, mantle length (mm), body weight (g), eye leans diameter (MM), and age (days). S = south, SM = southern middle, NM = northern middle, N = north.

Zone	Specimen ID Code	Station	Region	Year	Sex	Mantle Length (mm)	Body Weight (g)	Eye-Lens Diameter (mm)	Age (days)
3	BM049	SMP171 505054	S	2015	M	272	260	4.5	320
3	BM108	SMP171 505057	S	2015	M	193	79	4.6	329
3	BM109	SMP171 505057	S	2015	M	205	118	4.2	323
3	BM111	SMP171 505057	S	2015	M	288	207	4.6	343
3	BM113	SMP171 505057	S	2015	M	188	83	4.4	316
3	BM117	SMP171 505057	S	2015	F	186	117	4.5	296
3	BM118	SMP171 505057	S	2015	F	199	128	4.4	298
3	BM119	SMP171 505057	S	2015	F	193	121	4.3	271
3	BM120	SMP171 505057	S	2015	F	174	87	4.1	381
3	BM121	SMP171 505057	S	2015	F	155	90	3.7	324
4	BM070	SMP171 505053	SM	2015	F	182	121	4.2	351

Table 1 (Continued)

Zone	Specimen ID Code	Station	Region	Year	Sex	Mantle Length (mm)	Body Weight (g)	Eye-Lens Diameter (mm)	Age (days)
4	BM071	SMP171 505053	SM	2015	M	170	88	4.4	296
4	BM081	SMP171 505052	SM	2015	M	188	121	4.1	424
4	BM082	SMP171 505052	SM	2015	M	218	217	5.6	321
4	BM083	SMP171 505052	SM	2015	F	149	89	4.1	291
4	BM084	SMP171 505052	SM	2015	M	140	81	4.1	240
4	BM092	SMP171 505048	SM	2015	M	190	97	4.3	271
4	BM093	SMP171 505048	SM	2015	F	142	68	4.2	410
4	BM103	SMP171 505048	SM	2015	F	140	75	3.9	310
4	BM104	SMP171 505048	SM	2015	F	142	76	4.2	237
5	BM004	SMP171 505032	NM	2015	F	175	100	4.5	280
5	BM005	SMP171 505032	NM	2015	M	141	68	4.5	273
5	BM039	SMP171 505035	NM	2015	M	165	75	4.1	263
5	BM094	SMP171 505036	NM	2015	M	275	182	4.7	287
5	BM095	SMP171 505036	NM	2015	F	200	160	4.8	293
5	BM130	SMP171 505039	NM	2015	F	125	64	3.9	303
5	BM131	SMP171 505039	NM	2015	F	152	89	4.2	297
5	BM134	SMP171 505039	NM	2015	M	152	89	4.7	260
6	BM025	SMP171 505024	N	2015	M	170	98	4.3	349
6	BM037	SMP171 505025	N	2015	M	205	157	4.3	221
6	BM038	SMP171 505025	N	2015	M	139	70	4.0	288

Table 1 (Continued)

Zone	Specimen ID Code	Station	Region	Year	Sex	Mantle Length (mm)	Body Weight (g)	Eye-Lens Diameter (mm)	Age (days)
6	HS214	SMP171 904004	N	2019	M	238	148	4.3	324
6	HS215	SMP171 904004	N	2019	F	204	165	5.0	292
6	HS216	SMP171 904004	N	2019	F	191	121	4.4	315
6	HS217	SMP171 904004	N	2019	F	191	132	5.3	293
6	HS218	SMP171 904004	N	2019	F	191	114	4.6	316
6	HS219	SMP171 904004	N	2019	F	196	94	5.0	338
	Means				184	115	4.4	307	
	Standard Errors					6.31	7.50	0.063	6.99
	Coefficients of Variance				20.8	39.8	8.73	13.9	

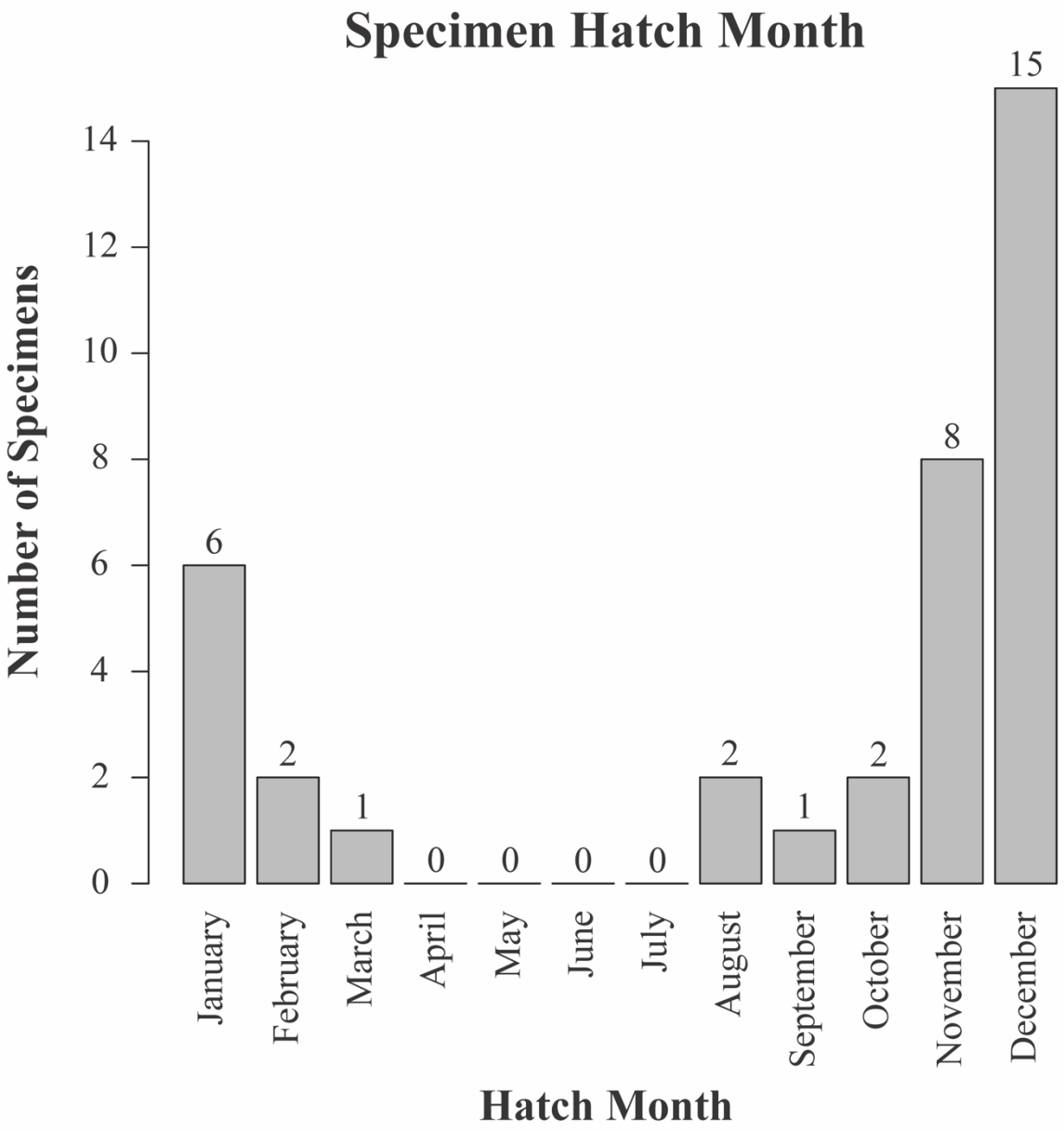

Figure 3. Specimen hatch month frequency histogram.

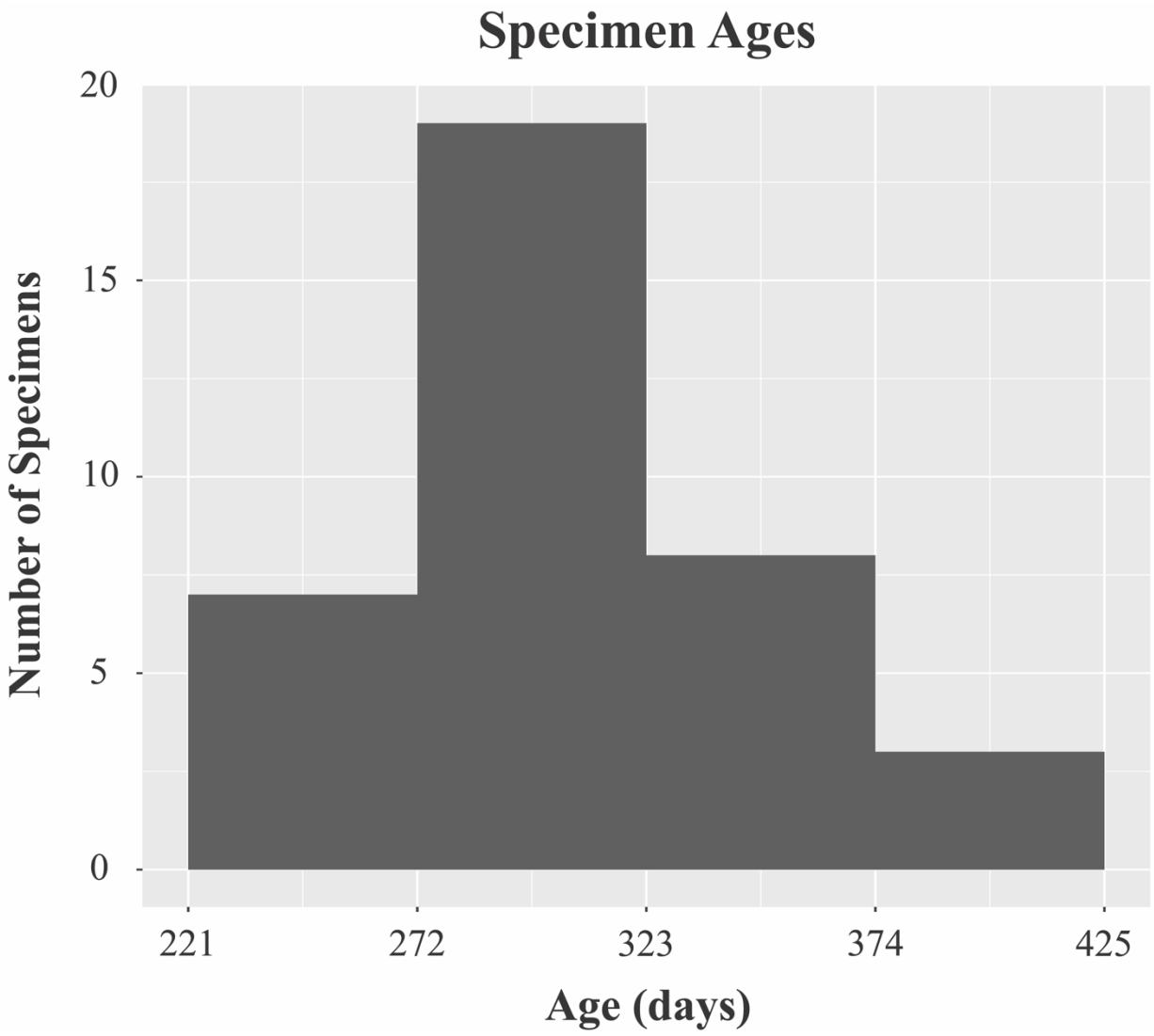

Figure 4. Specimen age distribution frequency histogram. Overall specimen age range binned into four equal age ranges.

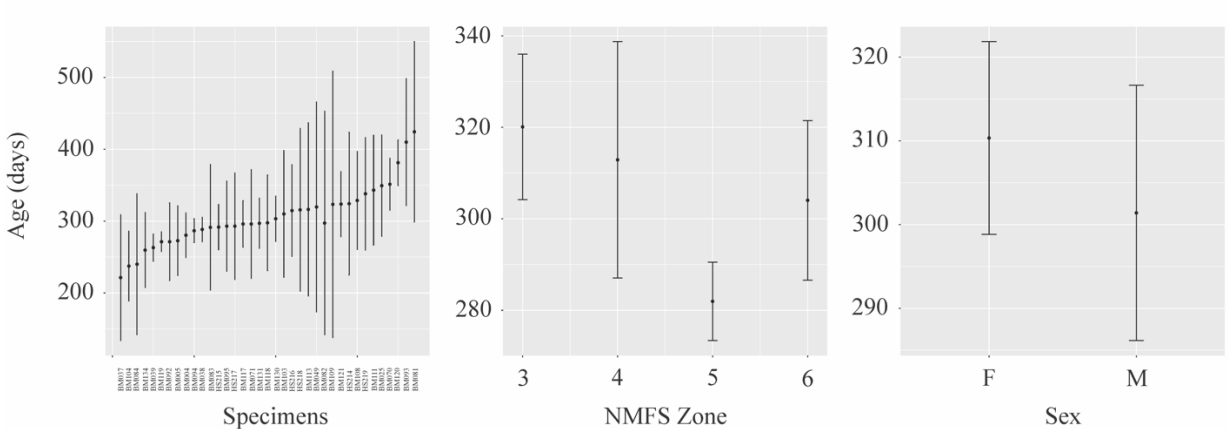

Figure 5. Age precision analysis. All three age estimates per specimen were used as individual data values. Mean ages are plotted by specimen (left), NMFS zone (center), and sex (right). Error bars show 95% confidence intervals.

III. RESULTS

III.I Statolith analyses

Specimen ages ranged between 221 and 424 days (7.3 to 13.9 months; one month is 30.4 days), with a mean age of 306.6 days (10.1 months), a standard error of 6.99, and a coefficient of variance of 13.9 (Table 1). Figure 4 indicates the most common age range of specimens when binned into four equally sized age ranges was 272-323 days. A boxplot displaying median ages per zone with 95% confidence intervals indicated no significant difference in age range among zones 3-6 (Figure 6). Additionally, age precision analyses were completed using all three age estimates per specimen as individual data values. Means of individual age counts were plotted by specimen, zone, and sex, with 95% confidence intervals (Figure 5). This analysis indicated a significant difference in mean ages between zones 3 and 4, but otherwise no significant difference in mean age between zones or sex.

Spearman's rank correlations were run between age and mantle length ($R_S = 0.21$, p-value = 0.21), age and weight ($R_S = 0.13$, p-value = 0.45), and age and eye-lens diameter ($R_S = -0.05$, p-value = 0.77), but there was no significant correlation between any of these variable combinations. Due to high variation in individual growth rates, there is a poor relationship between age and mantle length or weight for *D. pealeii* (Brodziak & Macy, 1996), so no correlation between age and eye-lens diameter was expected either. A Kruskal-Wallace test indicated there was no significant difference in hatch month (converted to numerical values) between zones.

Out of 37 specimens, most (78%) were hatched during winter (November-January), with a modal hatch month of December (41%) (Figure 3). The remaining eight specimens hatched either between the months of August and October (14%) or between February and March (8%). These data suggest *D. pealeii* on the West Florida Shelf hatch over a protracted period of time (i.e., August-April). If the GoM *D. pealeii* population spawns in two intra-annual cohorts like the U.S. northeast population (Macy & Brodziak, 2001), then the specimens included in the present study would be considered part of the winter cohort.

III.II Stable isotope analyses

For each *D. pealeii* specimen, the $\delta^{13}C$ and $\delta^{15}N$ isotopic ratios for each eye-lens lamina were plotted against diametric lamina midpoint, as well as each other (Appendices A, B, C). These isotope ratios relate to an isotopic signature for the environment that the supporting primary producer was present in, prior to fractionation due a change in trophic position (Minagawa & Wada, 1984; McCutchan Jr et al., 2003). Ratios were then compared to carbon and nitrogen isoscapes for the West Florida Shelf as previously determined by Radabaugh et al. (2013, 2014) to investigate potential migration patterns over each individual's life history.

For ease of comparison between *D. pealeii* and *D. plei* migration patterns, the analysis of stable isotope data in this study was modeled after Meath (2017) with modifications to methods. Initially, linear regression models were fitted to the $\delta^{13}C$ and $\delta^{15}N$ stable isotope ratios against each eye-lens lamina midpoint for each specimen. It was apparent that many of the regressions in this study followed parabolic (polynomial) rather than linear trends found in the study performed by Meath (2017) for *D. plei*. Therefore, rather than adhering to linear isotopic trends for all

specimens such as in Meath (2017), the methods were modified for the purposes of this study. Parabolic trends were included for both $\delta^{13}C$ and $\delta^{15}N$ to account for specimens that may have migrated at various rates over their lifetimes (e.g., stayed in one area for an extended period early in their lives then migrated to another location once mature, or vice versa).

To account for any possible parabolic trends, all $\delta^{13}C$ and $\delta^{15}N$ regressions for each specimen were first run on second-order polynomials. If the second term of the polynomial was not significant ($p > 0.05$, meaning it was not parabolic), it was removed and a linear regression model was utilized. Significant polynomials representing parabolic trends were reduced to linear regressions to determine whether the overall (first order) slope of the trend was positive or negative. If the resulting linear model was not significant, the polynomial was considered neutral. These regressions for $\delta^{13}C$ and $\delta^{15}N$ were compiled into output tables (Tables 2, 3; Appendices A, B) to compare trends and patterns in life history (Figure 7).

For $\delta^{13}C$ versus $\delta^{15}N$, Spearman's rank correlation was used for analysis because the data were not normally distributed (Table 4, Appendix C). This analysis also removes any arithmetic weight in values of tail distribution and is a more conservative analysis.

Core values of $\delta^{13}C$ and $\delta^{15}N$ from eye-lenses represent the earliest record we have of these isotopes for each specimen during their life history. *D. pealeii* eye-lenses begin forming prior to hatching (Arnold, 1966). Core values were excluded from all regression analyses due to the possibility of interference by maternal contribution to embryonic isotopes. Carbon stable isotope ratios, in particular, appeared to possibly be influenced by this potential effect (Figure 8). Radial lamina midpoint of eye-lens cores used in this study averaged 0.3 mm and *D. pealeii* paralarvae have an average mantle length of 1.8 mm upon hatching (J. J. McMahon & Summers,

1971). Multiple statistical tests were run for both $\delta^{13}C$ and $\delta^{15}N$ core values only. $\delta^{13}C$ and $\delta^{15}N$ eye-lens core values were plotted to visualize the potential of maternal contribution (Figure 9).

A Kolmogorov-Smirnov test for $\delta^{15}N$ core values versus zone indicated $\delta^{15}N$ cores were not normally distributed (p-value > 0.05), with a *p*-value of 0.11. A Kolmogorov-Smirnov test was also run for $\delta^{13}C$ core values, which resulted in a *p*-value of 0.82, indicating these data were also not normally distributed. The results of the Kolmogorov-Smirnov tests indicated a nonparametric test should be used for both core isotope values. A Kruskal-Wallis ANOVA for $\delta^{15}N$ core values versus zone resulted in a test statistic of 14.11 and a *p*-value of 0.003. This indicated the $\delta^{15}N$ core values for at least one zone were significantly different from the rest (95% confidence intervals), so a Bonferroni test was run (95% confidence intervals). Pairwise comparisons were made between average ranks of $\delta^{15}N$ core values for all four zones, and there was a significant difference between zones 3 and 6 for $\delta^{15}N$ core values versus zone. There was no significant difference between any other zone combination for $\delta^{15}N$ core values versus zone, and there was no significant difference between zones for $\delta^{13}C$ core values.

Figure 7 presents the migration trends of *D. pealeii* on the West Florida Shelf represented by each combination of $\delta^{13}C$ and $\delta^{15}N$ isotope trends (Appendices A, B). Most (81%; 14 male, 16 female) specimens exhibited a significant ($p \leq 0.05$) positive trend in $\delta^{13}C$ regressions against eye-lens lamina midpoint, indicating $\delta^{13}C$ increased throughout those specimens' lifespans (Table 2; Figure 7; Appendices A, B). On the West Florida Shelf, a positive $\delta^{13}C$ trend suggests inshore movement (i.e., movement eastward on the West Florida Shelf) as individuals age, because higher $\delta^{13}C$ values occur inshore, due to an increased importance of benthic microalgae as a basal resource in clear, shallow waters (Stowasser et al., 2006; Radabaugh et al., 2013; Radabaugh & Peebles, 2014). A negative $\delta^{13}C$ regression against eye-lens lamina midpoint

suggests a decrease in $\delta^{13}C$ and offshore movement over time (i.e., movement westward on the West Florida Shelf). A negative $\delta^{13}C$ trend was found in only one specimen (a male). The neutral, constant, or non-significant $\delta^{13}C$ trends don't necessarily suggest either inshore or offshore overall movement during the individual's lifetime. These trends could be due to an individual displaying inconsistent movement over the course of its lifetime (e.g., stationary for some time then moving, or inshore movement early in the individual's life and offshore movement later on, or vice versa) during its lifetime. Three specimens (8%; one male, two females) had a neutral $\delta^{13}C$ trend, and another three (8%; two males, one female) had no significant $\delta^{13}C$ trend.

Higher $\delta^{15}N$ values are present in the northern part of the GoM due to closer proximity to nitrogen inputs via the Mississippi and other rivers (Radabaugh et al., 2013; Radabaugh & Peebles, 2014). When looking at $\delta^{15}N$ plotted against eye-lens lamina midpoint, a positive trend suggests northward movement along the West Florida Shelf. A positive $\delta^{15}N$ trend was found in 14 out of 37 specimens (38%; six male, eight female; northward movement), which accounts for one third of the males included in this study and over one third of the females included (Table 3). A negative $\delta^{15}N$ trend in the GoM suggests southward movement overall during the squids' lifetime, which was found in nine specimens (24%; four male, five female). A neutral trend neither suggests northward nor southward movement in the GoM, and was found in six specimens (16%; three male, three female). No significant $\delta^{15}N$ trend does not indicate either northward or southward movement overall during the squids' lifetime. Eight specimens had no significant $\delta^{15}N$ trend (five male, three female). This could be due to inconsistent movement over the specimens' lifetime, or potentially a combination of moving northward and southward during different periods in the squids' lifetime.

A schematic of individual-specific migration paths inferred from the stable isotope analyses of the *D. pealeii* specimens included in this study was produced, including migration patterns broken down by zone, as well as migration patterns for *D. plei* found by Meath et al. (2019) (Figure 7). Of the ten squid in zone 3 (the southernmost zone), four moved straight east (path 3); two moved either east or west with no known north or south movement (path 1); two moved northeast (path 8); one moved either south, southeast, or southwest (path 4); and one moved either south or southeast (path 6). Of the ten squid in zone 4 (the southern middle zone), five moved northeast (path 8); four moved straight east (path 3); and one moved either north, northeast, or northwest (path 5). Of the 8 squid in zone 5 (the northern middle zone), five moved northeast (path 8); two moved straight east (path 3); and one moved southwest (path 9). Of the 9 squid in zone 6 (the northernmost zone), four moved either south or southeast (path 6); two moved straight east (path 3); two moved either south, southeast, or southwest (path 4); and one moved northeast (path 8).

Because 81% of specimens had a positive $\delta^{13}C$ trend, it was difficult to tell if different $\delta^{13}C$ trends could potentially be related to differences in mantle length, weight, eye-lens diameter, age, or hatch month. There was no significant difference in mantle length, weight, eye-lens diameter, or age among any of the different $\delta^{15}N$ trends observed in this study.

For $\delta^{13}C$ vs. $\delta^{15}N$ Spearman's rank correlations (Table 4, Appendix C), 13 specimens (35%) had a positive correlation between $\delta^{13}C$ and $\delta^{15}N$, four (11%) had a negative correlation, and 20 (54%) had no significant correlation (Table 4). A high positive correlation between $\delta^{13}C$ vs. $\delta^{15}N$ along the West Florida Shelf can either be indicative of trophic growth (e.g., consuming prey at progressively higher trophic positions) with minimal movement over the specimen's lifespan, or northeast movement. Significant negative correlations suggest overall southeast

movement. See also Figure 7 for more details on individual migration patterns, as all isotope data must be viewed together to understand each specimens' movement pattern over their individual lifespan.

III.III Migration patterns related to life history

Due to the current methodology of separating eye-lens laminae, it was not possible to correlate statolith-based specimen age data to eye-lens diameter. Individual eye-lens layers (much smaller than the laminae used in this study – which are actually groups of individual layers) would be too small of an amount to conduct stable isotope analysis (and too small to see with the naked eye or separate individually) with the current technology available. In addition, the rate at which individual eye-lens layers form is currently unknown for this species, and the current delamination methods are not accurate enough to separate the same amount of eye-lens layers within each lamina each time. Therefore, it is not possible to directly compare age to the number of eye-lens laminae. Additionally, due to the variable growth rates in squid (e.g., with changes in temperature and food consumption, as previously mentioned), it is also not possible to directly compare age to eye-lens diameter. Instead, the most reliable method was used – statolith increment counts. Capture date and age were then used to back-calculate hatch month of each individual (Figure 3). The migration patterns for the GoM *D. pealeii* population were qualitatively compared to those of the northeastern *D. pealeii* population (e.g., general inshore-offshore and north-south movements) (Summers, 1969; Cadrin, 1998; Jacobson, 2005).

Boxplots of mantle length, weight, and eye-lens diameter per zone are provided in Figure 6, and Kruskal-Wallace tests were run to determine if there was any significant difference in

these variables among zones. Across all four zones, there was no significant difference in squid weight. There was also no significant difference in eye-lens diameter across zones. A Kruskal-Wallace test indicated there was a significant difference in mantle lengths across zones with a *p*-value of 0.046. A Dunn test indicated there was a significant difference in mantle length between zones 3 and 4 (the two southern zones, *p*-value = 0.0184), as well as between zones 4 and 6 (the southern middle zone and the northern zone, *p*-value = 0.0486). Otherwise, there were no significant differences in mantle length among zones.

III.IV Migration patterns of *D. pealeii* and *D. plei*

Figure 7 includes the inferred migration patterns for each combination of stable isotope data ($\delta^{13}C$ vs diametric lamina midpoint, $\delta^{15}N$ vs diametric lamina midpoint, and $\delta^{13}C$ vs $\delta^{15}N$ trends). Tallies from Meath (2019) and this study were aligned, allowing for comparison of the migration patterns between *D. pealeii* and *D. plei*. In Figure 7, positive isotope trends are referred to as "increasing," negative trends are "decreasing," and neutral or not significant trends are "constant." Data for *D. plei* was provided by Meath et al. (2019). Path 1 (constant $\delta^{13}C$, constant $\delta^{15}N$) suggests general movement either east or west along the same latitude. Two *D. pealeii* specimens included in this study had this pattern, and three *D. plei* specimens exhibited this pattern. Path 2 (decreasing $\delta^{13}C$, constant $\delta^{15}N$) suggests overall westward movement into deeper waters, which was exhibited by no *D. pealeii* and one *D. plei* specimen. Path 3 (increasing $\delta^{13}C$, constant $\delta^{15}N$) implies general eastward movement inshore to shallower waters, which was observed in 12 *D. pealeii* and ten *D. plei* specimens. Path 4 (constant $\delta^{13}C$, decreasing $\delta^{15}N$) indicates either southward, southeastward, or southwestward movement, and was observed

in three *D. pealeii* and no *D. plei* specimens. Path 5 (constant $\delta^{13}C$, increasing $\delta^{15}N$) suggests either northward, northeastward, or northwestward movement, which was displayed by one *D. pealeii* and eight *D. plei*. Path 6 (increasing $\delta^{13}C$, decreasing $\delta^{15}N$) supports either southward or southeastward movement, and was observed in five *D. pealeii* and no *D. plei*. Path 7 (decreasing $\delta^{13}C$, increasing $\delta^{15}N$) indicates either northward or northwestward movement, and was found in no *D. pealeii* and four *D. plei*. Path 8 (increasing $\delta^{13}C$, increasing $\delta^{15}N$) implies northeastward movement, displayed by 13 *D. pealeii* and 16 *D. plei*. Path 9 (decreasing $\delta^{13}C$, decreasing $\delta^{15}N$) suggests overall southwestward movement and was only found in one *D. pealeii* specimen and no *D. plei* specimens.

The highest numbers of *D. pealeii* (35%) and *D. plei* (38%) were found to have patterns of northeastward movement. The second highest numbers of both populations (32% *D. pealeii*, 24% *D. plei*) were observed to have an overall eastward movement over their lifetime to shallower waters. Together, these two migration patterns (northeastward and eastward) account for 68% of *D. pealeii* specimens observed in this study and 62% of *D. plei* observed by Meath et al. (2019). The third highest number of *D. pealeii* observed in this study (14%) migrated either southward or southeastward over the course of the specimens' lifetimes. The third highest number of *D. plei* (19%) had either northward, northeastward, or northwestward movement with no evidence of moving south. Due to the high variability of results, it is recommended that a much larger sample size be used in the future in order to best represent the population.

III.V Tables and Figures

Table 2. $\delta^{13}C$ and diametric eye-lens lamina midpoint isotope regression trends. For parabola orientation, convex opens upward, concave opens downward, and NS is not significant (p values < 0.05 considered significant).

Zone	Specimen ID Code	$\delta^{13}C$ Parabola Orientation or Linear	$\delta^{13}C$ Trend	$\delta^{13}C$ *p* value	$\delta^{13}C$ R^2	$\delta^{13}C$ Adjusted R^2	Laminae Count (n)
3	BM049	Concave	Neutral	0.022	42.11	33.84	17
3	BM108	Linear	Positive	<0.001	81.27	79.56	13
3	BM109	Linear	Positive	0.003	65.00	61.11	11
3	BM111	NS	NS	0.59	1.81	-4.33	18
3	BM113	Convex	Positive	<0.001	82.80	79.93	15
3	BM117	Linear	Positive	<0.001	78.50	76.35	12
3	BM118	Convex	Positive	<0.001	78.43	74.83	15
3	BM119	Concave	Positive	0.006	67.45	60.21	12
3	BM120	Concave	Neutral	0.033	53.20	42.80	12
3	BM121	Linear	Positive	0.022	54.91	48.47	9
4	BM070	Linear	Positive	<0.001	86.21	85.06	14
4	BM071	Linear	Positive	<0.001	87.47	86.22	12
4	BM081	Linear	Positive	<0.001	88.05	86.85	12
4	BM082	Linear	Positive	0.002	59.39	55.70	13
4	BM083	Linear	Positive	0.004	52.27	48.30	14
4	BM084	Linear	Positive	<0.001	86.10	85.11	16
4	BM092	Convex	Positive	<0.001	94.57	93.48	13
4	BM093	NS	NS	0.71	1.11	-6.50	15
4	BM103	Linear	Positive	<0.001	84.04	82.27	11
4	BM104	Convex	Positive	<0.001	82.76	78.92	12
5	BM004	Convex	Positive	<0.001	78.74	75.47	16
5	BM005	Concave	Positive	0.008	66.22	58.71	14
5	BM039	Concave	Negative	0.002	74.00	68.66	14
5	BM094	Convex	Positive	<0.001	87.57	85.49	15
5	BM095	Linear	Positive	<0.001	82.70	81.74	20
5	BM130	Linear	Positive	<0.001	70.62	68.17	14
5	BM131	Linear	Positive	<0.001	88.29	87.22	13

Table 2 (Continued)

Zone	Zone	Zone	Zone	Zone	Zone	Zone	Zone
5	BM134	Convex	Positive	<0.001	81.44	78.79	17
6	BM025	Concave	Positive	0.003	68.98	62.78	13
6	BM037	Linear	Positive	<0.001	80.34	78.15	11
6	BM038	Linear	Positive	<0.001	92.84	91.95	10
6	HS214	NS	NS	0.73	2.11	-14.21	8
6	HS215	Linear	Positive	<0.001	78.39	76.95	17
6	HS216	Concave	Positive	0.001	68.95	63.77	15
6	HS217	Linear	Positive	<0.001	73.81	71.19	12
6	HS218	Convex	Positive	<0.001	78.86	75.34	15
6	HS219	Concave	Neutral	0.003	61.89	55.54	15

Table 3. $\delta^{15}N$ and diametric eye-lens lamina midpoint isotope regression trends. For parabola orientation, convex opens upward, concave opens downward, and NS is not significant (*p* values < 0.05 considered significant).

Zone	Specimen ID Code	$\delta^{15}N$ Parabola Orientation or Linear	$\delta^{15}N$ Trend	$\delta^{15}N$ *p* value	$\delta^{15}N$ R^2	$\delta^{15}N$ Adjusted R^2	Laminae Count (n)
3	BM049	NS	NS	0.21	10.20	4.22	17
3	BM108	NS	NS	0.66	1.80	-7.13	13
3	BM109	Linear	Positive	0.005	59.48	54.98	11
3	BM111	Linear	Negative	0.020	30.49	26.15	18
3	BM113	Linear	Negative	<0.001	79.51	77.94	15
3	BM117	Convex	Neutral	0.010	64.12	56.14	12
3	BM118	Convex	Neutral	0.011	53.15	45.34	15
3	BM119	NS	NS	0.27	12.18	3.40	12
3	BM120	Concave	Neutral	0.024	56.41	47.73	12
3	BM121	Concave	Positive	<0.001	92.85	90.47	9
4	BM070	NS	NS	0.066	25.35	19.13	14
4	BM071	NS	NS	0.90	0.17	-9.81	12
4	BM081	NS	NS	0.21	15.21	6.73	12
4	BM082	Concave	Positive	0.003	67.92	61.51	13
4	BM083	Convex	Positive	<0.001	92.95	91.66	14
4	BM084	Convex	Neutral	0.046	37.72	28.13	16
4	BM092	Convex	Positive	0.001	76.06	71.27	13
4	BM093	Linear	Positive	<0.001	65.45	62.79	15

Table 3 (Continued)

Zone	Specimen ID Code	$\delta^{15}N$ Parabola Orientation or Linear	$\delta^{15}N$ Trend	$\delta^{15}N$ *p* value	$\delta^{15}N$ R^2	$\delta^{15}N$ Adjusted R^2	Laminae Count (n)
4	BM103	Linear	Positive	0.052	35.71	28.56	11
4	BM104	Linear	Positive	0.009	50.70	45.77	12
5	BM004	NS	NS	0.35	6.28	-0.41	16
5	BM005	Linear	Positive	0.040	35.83	29.41	14
5	BM039	Concave	Negative	<0.001	91.00	88.66	14
5	BM094	Convex	Neutral	0.001	72.15	67.51	15
5	BM095	Linear	Positive	<0.001	83.28	82.35	20
5	BM130	Linear	Positive	<0.001	80.70	79.09	14
5	BM131	Linear	Positive	0.004	55.43	51.38	13
5	BM134	Linear	Positive	<0.001	65.94	63.67	17
6	BM025	NS	NS	0.97	0.01	-9.08	13
6	BM037	Concave	Positive	0.009	69.36	61.70	11
6	BM038	Concave	Neutral	0.019	67.69	58.46	10
6	HS214	Linear	Negative	<0.001	91.57	90.16	8
6	HS215	Concave	Negative	<0.001	94.03	93.17	17
6	HS216	Linear	Negative	0.001	55.89	52.50	15
6	HS217	Concave	Negative	<0.001	97.09	96.44	12
6	HS218	Concave	Negative	0.004	60.50	53.91	15
6	HS219	Convex	Negative	<0.001	81.35	78.25	15

Table 4. $\delta^{13}C$ vs. $\delta^{15}N$ isotope regression trends using Spearman's correlation. Regressions found to be not significant are labeled NS (*p* values < 0.05 considered significant).

Zone	Specimen ID Code	$\delta^{15}N$ vs. $\delta^{13}C$ Spearman's rank correlation R_S value	$\delta^{15}N$ vs. $\delta^{13}C$ Spearman's rank correlation p value	$\delta^{15}N$ vs. $\delta^{13}C$ significant linear regression slopes
3	BM049	0.21	0.41	NS
3	BM108	0.24	0.40	NS
3	BM109	0.74	0.020	0.596
3	BM111	-0.17	0.47	NS
3	BM113	-0.79	0.003	-0.298
3	BM117	-0.36	0.23	NS
3	BM118	0.89	<0.001	0.654
3	BM119	0.62	0.039	0.507

Table 4 (Continued)

Zone	Specimen ID Code	$\delta^{15}N$ vs. $\delta^{13}C$ Spearman's rank correlation R_S value	$\delta^{15}N$ vs. $\delta^{13}C$ Spearman's rank correlation p value	$\delta^{15}N$ vs. $\delta^{13}C$ significant linear regression slopes
3	BM120	0.55	0.070	NS
3	BM121	0.45	0.20	NS
4	BM070	0.60	0.030	0.163
4	BM071	-0.22	0.47	NS
4	BM081	0.52	0.090	NS
4	BM082	0.67	0.020	0.837
4	BM083	0.79	0.004	0.581
4	BM084	0.20	0.44	NS
4	BM092	0.75	0.009	0.352
4	BM093	-0.15	0.58	NS
4	BM103	0.55	0.080	NS
4	BM104	0.96	0.002	0.816
5	BM004	-0.01	0.96	NS
5	BM005	0.48	0.080	NS
5	BM039	0.71	0.010	1.353
5	BM094	0.49	0.070	NS
5	BM095	0.84	0.003	1.27
5	BM130	0.81	0.004	0.343
5	BM131	0.70	0.015	0.352
5	BM134	0.82	0.001	0.949
6	BM025	-0.03	0.91	NS
6	BM037	0.54	0.080	NS
6	BM038	0.11	0.75	NS
6	HS214	-0.12	0.75	NS
6	HS215	-0.79	0.002	-1.452
6	HS216	-0.37	0.16	NS
6	HS217	-0.84	0.006	-1.624
6	HS218	-0.61	0.023	-1.239
6	HS219	-0.03	0.91	NS

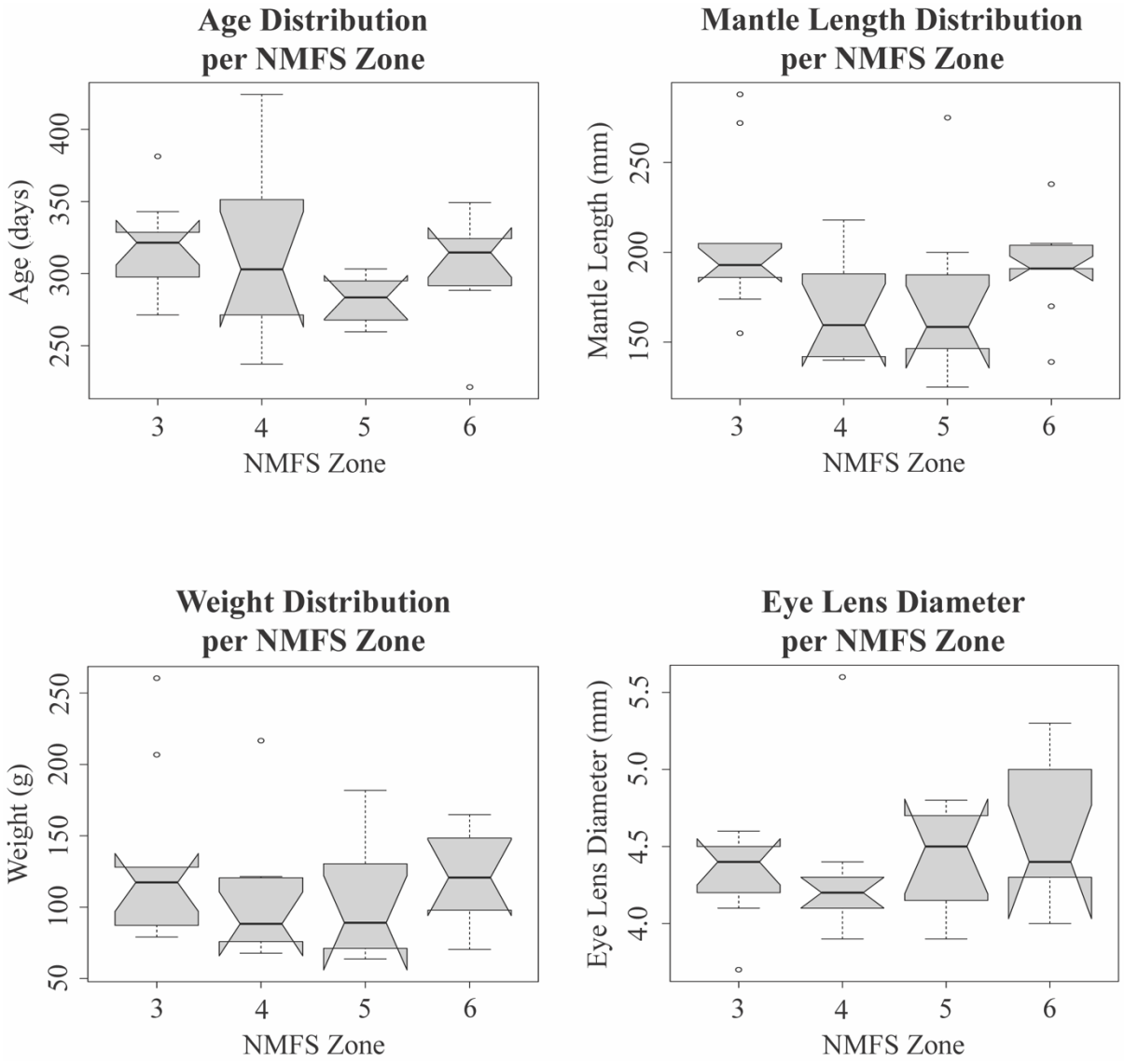

Figure 6. Boxplots of age (days), mantle length (mm), weight (g), and eye-lens diameter (mm) per zone. Medians are represented within each box, box borders represent first and third quartiles, dotted lines represent minimums and maximums, outliers are represented by circles, and notches represent 95% confidence intervals for the meadian.

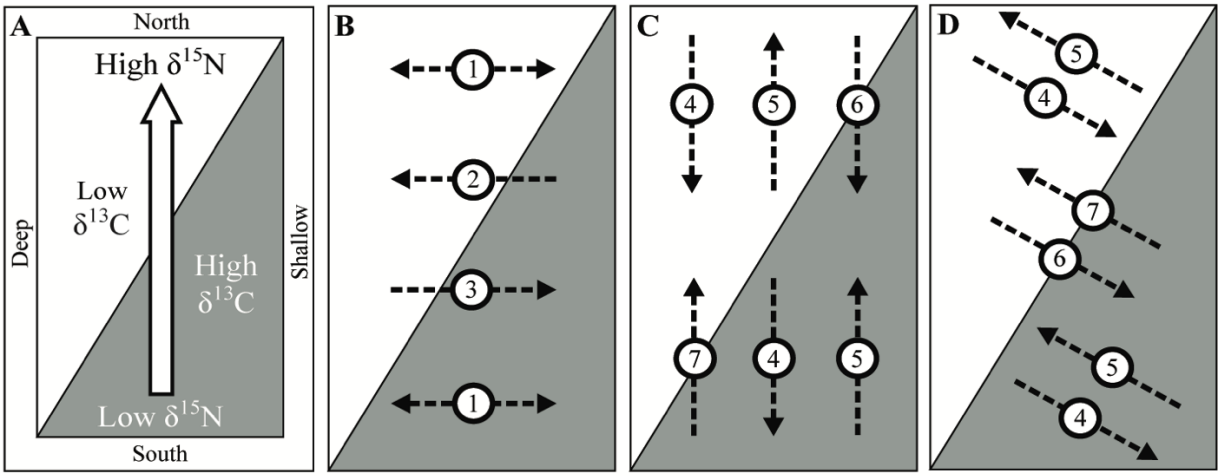

	Stable Isotope Trends		*D. pealeii*					*D. plei*
Path	$\delta^{13}C$	$\delta^{15}N$	Zone 3	Zone 4	Zone 5	Zone 6	Total	Total
1	constant	constant	2	0	0	0	2	3
2	decreasing	constant	0	0	0	0	0	1
3	increasing	constant	4	4	2	2	12	10
4	constant	decreasing	1	0	0	2	3	0
5	constant	increasing	0	1	0	0	1	8
6	increasing	decreasing	1	0	0	4	5	0
7	decreasing	increasing	0	0	0	0	0	4
8	increasing	increasing	2	5	5	1	13	16
9	decreasing	decreasing	0	0	1	0	1	0

Figure 7. Migration pattern tallies according to stable isotope trends. Positive trends are referred to as "increasing," negative trends are "decreasing," and neutral or not significant trends are "constant." A: Legend with cardinal directions and overall $\delta^{13}C$ and $\delta^{15}N$ isoscapes present on the West Florida Shelf. B-E: Inferred migration patterns for each path listed in the table. Data for *D. plei* provided by Meath (2019) for comparison.

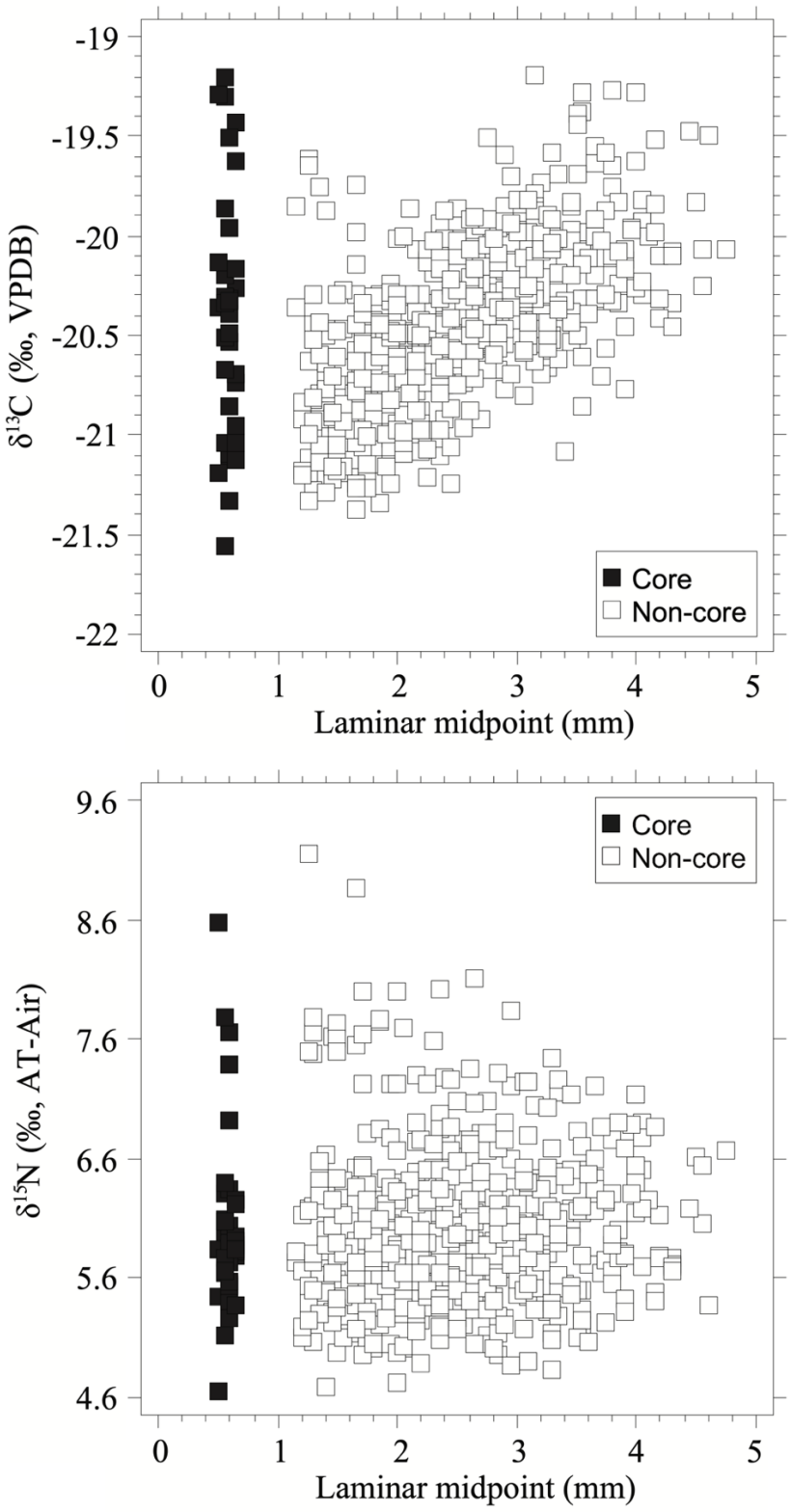

Figure 8. Scatterplots of $\delta^{13}C$ and $\delta^{15}N$ values with eye-lens laminar midpoint for all specimens. Diametric laminar midpoints were used for all laminae accept eye-lens cores. Radial laminar midpoints were used for eye-lens cores.

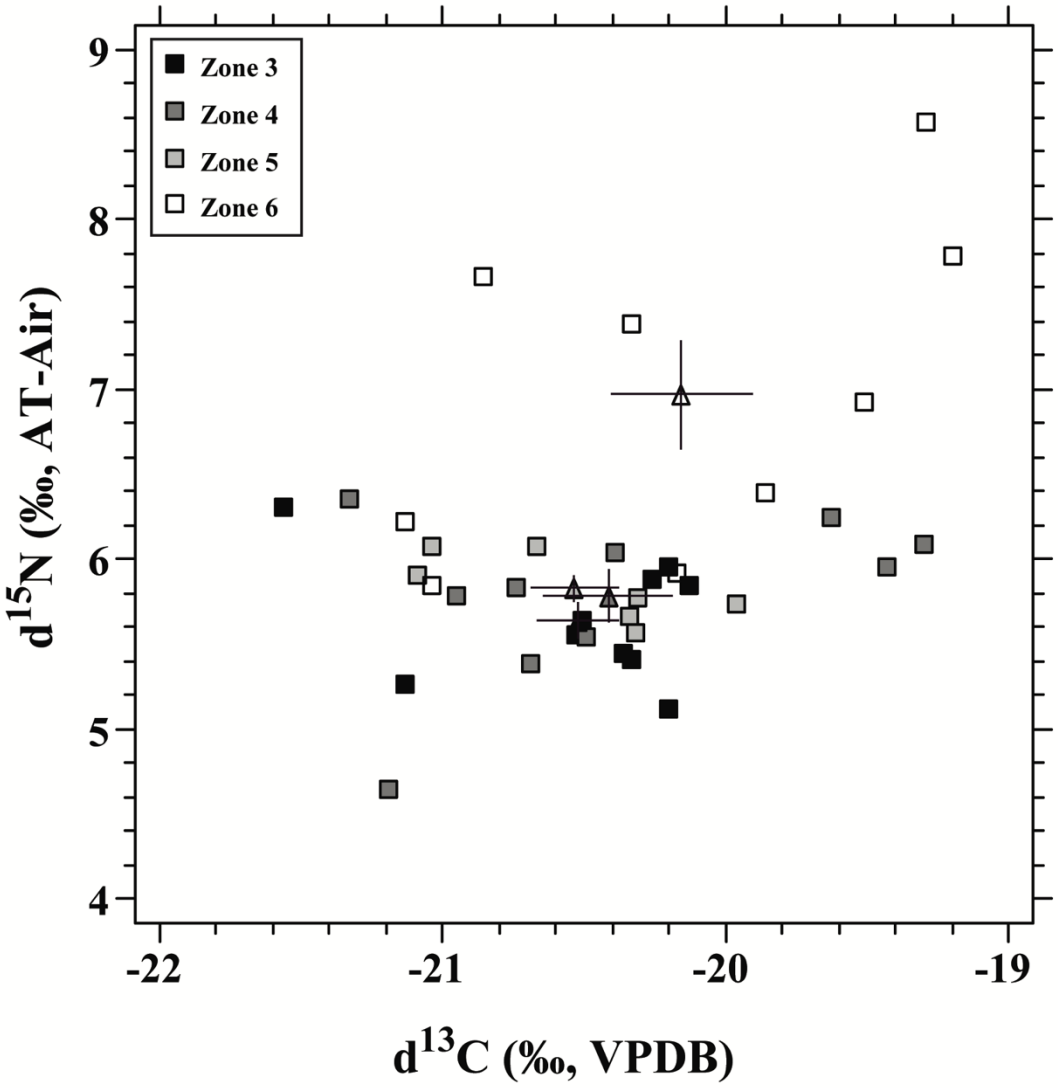

Figure 9. $\delta^{13}C$ vs. $\delta^{15}N$ eye-lens core values. Error bars for each zone (centered with color coded triangles) are based on means and standard errors.

IV. DISCUSSION

IV.I Ages of GoM *D. pealeii*

Statolith-based age determination is the most widely used method of assessing squid age for cohort identification, as well as estimation of population growth rates and median size-at-maturity because these methods are considered to be the most reliable (Arkhipkin & Shcherbich, 2012). The mean age of the squid in this study (306 days, 10.1 months) is within the known age range of the northeast *D. pealeii* population, which is less than one year old (Brodziak & Macy, 1996; Hatfield et al., 2001; Macy & Brodziak, 2001). The maximum age observed in this study was 424 days, or 13.9 months.

Three specimens (8%; BM120, BM093, and BM081) were observed to be greater than one year old, all with hatch dates in the months of August and September. The precision analysis plot of average age by specimen is shown in Figure 5. The 95% confidence intervals for both BM093 and BM081 are both within the range for specimens aging 300-325 days. Additionally, BM120 – aged 381 days – has a lower confidence interval than over half of the other specimens. Therefore, the age estimates for these three squid may be accurate even though they are outside the currently accepted age range of under one year for this species (Macy, 1995; Brodziak & Macy, 1996; Hatfield et al., 2001; Macy & Brodziak, 2001; Hatfield & Cadrin, 2002; Jacobson, 2005; Jereb & Roper, 2010). This could possibly be due to the differences in water temperature between the GoM population and the northeast population (Serchuk & Rathjen, 1974; Love et al., 2013; Arkhipkin et al., 2015). This species is known to grow at a faster rate with an increase

in water temperature as low as 5°C (Hatfield et al., 2001; Forsythe, 2004). However, relationships between length and age, and weight and age, are not reliable for this species (Brodziak & Macy, 1996). Individual growth rates show high plasticity for most squid species.

The *D. pealeii* specimens included in this study hatched over a protracted period, between the moths of August and April. This aligns with the spawning of the northeast population's winter cohort (Macy & Brodziak, 2001). It is likely that spawning occurs over a broader period of time for the GoM population of *D. pealeii* than observed in this study, but sampling solely in the month of October likely limited specimens used here to only include the winter cohort.

IV.II Migration patterns of *D. pealeii* and Life History Correlations

There was a significant difference in mantle length between zones 3 and 4 (the two southernmost zones) as well as between zones 4 and 6 (the southern middle zone and the northern zone). Mean sea surface temperature only changes approximately two degrees Celsius across this study area (Love et al., 2013), so this difference is not likely due to a difference in sea surface temperature (Forsythe, 2004; Love et al., 2013). There is no significant difference in age range between the four zones, so this is not likely due to a difference in hatch month, but instead likely due to the small sample size, as well as the selection of larger specimens in order to conduct a more comprehensive stable isotope analysis. Eye-lens laminae sample weights for stable isotope analysis were between 300 – 600 µg, in accordance with Meath (2017), resulting in eye-lens cores being delaminated to no smaller than 1.0 mm in diameter. This is a limitation of current mass spectrometry methods, and as technology improves and smaller samples are able to be processed this method can provide a finer scale of resolution.

There is a clear difference in trends between $\delta^{13}C$ and $\delta^{15}N$ eye-lens core values and other laminae, which is thought to be due to maternal contribution. One study done on the loliginid *Loligo forbesi* mentioned that embryos of this species acquire trace metals from the yolk, which is derived solely from the mother (Craig, 2001). This study also stated that $\delta^{13}C$ vs. $\delta^{15}N$ ratios in *L. forbesi* did not have a significant decrease between the developmental stages of egg and hatchling (Craig, 2001). Other studies support the idea that not only do different tissues in cephalopods go through isotopic turnover at different rates (Hobson & Cherel, 2006; Jackson et al., 2007), but also that it is possible for fatty acids in certain tissues to reflect change in diet in as little as ten days in the loliginid squid *Lolliguncula brevis* (Stowasser et al., 2006).

Other cephalopods have also exhibited differences that are thought to be related to maternal contribution. Additionally, it is known that the youngest part of the *D. pealeii* eye-lens is formed prior to hatching (Arnold, 1966). For this reason, the eye-lens core laminae values were excluded from the lifelong stable isotope trends (Tables 2, 3, 4; Appendices A, B, C). This means that the eye-lens core values may provide insight into where the maternal parents of these individuals were before laying their eggs.

Eye-lens core $\delta^{13}C$ vs. $\delta^{15}N$ ratios were plotted with error bars for each zone (Figure 9). All zones except zone 6, the northernmost zone, seem to have their spawning grounds intermixed. The separation of zone 6 eye-lens core values suggests some degree of site fidelity in the northernmost zone, and that these squid are staying generally in the same areas and/or following the same migration patterns as their mothers.

Roughly half of *D. pealeii* specimens (54%) had $\delta^{13}C$ and $\delta^{15}N$ trends that suggested either northeastward or eastward movement over the course of their lifetimes. This suggests that

over half of the squid observed hatched offshore in deeper waters and migrated inshore to shallower waters, sometimes also moving northward at the same time.

The majority of specimens (78%) hatched between the months of November and January, and all specimens hatched between the months of August and March. For the northeast *D. pealeii* population, back-calculated hatch month data indicated the presence of two dominant intra-annual cohorts; winter-hatched and summer-hatched cohorts, with the latter occurring inshore and the winter spawning location being unidentified (Macy & Brodziak, 2001). The northeastern population migrates northward and inshore during the spring and south and offshore during late fall (Serchuk & Rathjen, 1974; Cadrin, 1998). This annual migration pattern was also inferred from the stable isotope analysis from the present study. Differences in hatch months between the GoM and northeastern populations could possibly be contributed to differences in water temperature (Love et al., 2013; Locarnini et al., 2019).

A study conducted along the Yucatan Shelf in the southeastern GoM found *D. plei* paralarvae to be most abundant at depths between 15 and 50 m, and from 21 to 163 km from the coastline (Guarneros-Narváez et al., 2022). The same study also found *D. plei* paralarvae abundance to be highest in early summer, followed by a decrease through late autumn (Guarneros-Narváez et al., 2022). However, *D. pealeii* specimens were not found in the samples, possibly due to the seasons in which samples were collected (i.e., July-November). The study results suggest other loliginid species in the GoM often hatch inshore during early summer – the exact opposite of what is suggested to occur with *D. pealeii* in the current study. *Doryteuthis pealeii* in the present study were only collected during the fall, and only specimens that were large enough for sufficient stable isotope trend analysis were selected, which could account for

this difference. A broader range in specimen size and collection seasonality could potentially produce different results.

The inferred migration patterns of the present study were based on the isoscapes determined by Radabaugh et al. (2013) and Radabaugh and Peebles (2014). Through the addition of isoscapes of the entire GoM, additional migration patterns for *D. pealeii* captured on the West Florida Shelf could be suggested (Le-Alvarado et al., 2021; Hernández-Sánchez et al., 2023). For example, a constant $\delta^{15}N$ trend could suggest a lack in northward or southward movement (as suggested in this study), but it could also suggest movement around the southern tip of Florida, east or west within the Florida Strait, due to similar $\delta^{15}N$ values in the isoscape along the southern coast (Le-Alvarado et al., 2021; Hernández-Sánchez et al., 2023). A decrease in $\delta^{15}N$ could suggest southward movement (as interpreted in this study), but it could also suggest movement offshore, away from the continental shelf and into the central GoM which is unlikely in this study because specimens were collected on the West Florida Shelf (Le-Alvarado et al., 2021). An increase in $\delta^{13}C$ could suggest eastward movement (suggested here), or in the southern half of this study area it could also suggest southward movement toward the Florida Strait if a constant distance from the coast is maintained (Le-Alvarado et al., 2021). In addition to movement offshore (westward from the coast, as suggested here), a decreasing $\delta^{13}C$ value could potentially indicate movement inshore from the central GoM onto the edge of the continental shelf, particularly close to where many of the zone 5 (northern middle zone) specimens were collected for this study (Le-Alvarado et al., 2021). A decrease in $\delta^{13}C$ could also suggest northward movement, depending on sampling location (Le-Alvarado et al., 2021).

Buresch et al. (2006) suggested there may be some movement of *D. pealeii* between the GoM and the northern population located along the northeastern coast of the United States. In

order to confirm or reject this suggestion, more research needs to be done on the $\delta^{13}C$ and $\delta^{15}N$ isoscapes connecting the two regions. Isoscapes of the Atlantic Ocean as a whole have been recorded on a more global scale (Graham et al., 2010; K. W. McMahon et al., 2013), but an isoscape with a higher resolution looking specifically at the area in question (GoM, through the Florida Strait, and up the eastern US coast) could provide more insight into this possibility. Also addressing this issue, a genetic study did find that there was a genetic break between the two *D. pealeii* populations located in the northern GoM and the Atlantic (Herke & Foltz, 2002).

All specimens used in this study were collected during October of both 2015 and 2019, so it is hard to draw definite conclusions about the spawning timeline relative to hatch month data of *D. pealeii* in the GoM. However, the data collected in this study does suggest spawning occurs over a protracted period here (Figure 3), similar to the two intra-annual cohorts of the northeastern *D. pealeii* population (Verrill, 1882; Cadrin, 1998; Macy & Brodziak, 2001; Hatfield & Cadrin, 2002; Shaw et al., 2010). A more comprehensive study would need to be conducted involving a larger sample size and year-round sampling in order to draw any definite conclusions about the spawning patterns of the *D. pealeii* stock within the GoM.

IV.III Migration patterns of *D. pealeii* and *D. plei*

On the West Florida Shelf, the majority of *D. pealeii* and *D. plei* specimens (Meath et al., 2019) – 54.0% and 61.9% respectively – had $\delta^{13}C$ and $\delta^{15}N$ trends that indicated either northeastward or eastward (i.e., both paths toward inshore) movements over the course of specimens' lifetimes. This study suggests the general migration patterns for the remaining individuals diverge from each other outside of these two most popular patterns. The fact that

over half of *D. pealeii* and *D. plei* specimens share the same general migration patterns would provide a possible explanation as to why these species are often captured together on the West Florida Shelf. Such similar migration patterns between these two species make it more difficult identify at sea.

IV.IV Future Research

For future studies, larger sample sizes collected during multiple times of the year for both species could provide a higher resolution of overall migration patterns. This would benefit future fisheries management of both species in the GoM, especially along the West Florida Shelf.

Until this study, little was known about the migration patterns of *D. pealeii* in the eastern GoM throughout their life history in comparison to populations located farther north along the eastern coast of the United States (Cadrin, 1998; Arkhipkin et al., 2015). Prior to the use of stable isotope analysis on eye-lenses, the literature lacked a reliable method for determining migration patterns throughout the life history of squid. Analyzing stable isotopes to determine species migration patterns is still a novel concept in comparison to traditional tagging methods, but the results of recent studies are promising and this type of analysis works with certain invertebrates as well as vertebrates (Radabaugh et al., 2013; Radabaugh & Peebles, 2014; Wallace et al., 2014; Meath et al., 2019). The combination of statolith and stable isotope analyses is a new, informative approach for the study of squid ecogeography and life history.

WORKS CITED

Arkhipkin, A. I. (2005). Statoliths as 'black boxes'(life recorders) in squid. *Marine and Freshwater Research, 56*(5), 573-583.

Arkhipkin, A. I., Rodhouse, P. G. K., Pierce, G. J., Sauer, W., Sakai, M., Allcock, L., . . . Zeidberg, L. D. (2015). World Squid Fisheries. *Reviews in Fisheries Science & Aquaculture, 23*(2), 92-252. doi:10.1080/23308249.2015.1026226

Arkhipkin, A. I., & Shcherbich, Z. N. (2012). Thirty years' progress in age determination of squid using statoliths. *Journal of the Marine Biological Association of the United Kingdom, 92*(6), 1389-1398.

Arnold, J. M. (1966). On the occurrence of microtubules in the developing lens of the squid Loligo pealii. *Journal of ultrastructure research, 14*, 534-539.

Bizikov, V. A. (1991). A new method of squid age determination using the gladius. *Squid age determination using statoliths*, 39-51.

Blainville, H. M. D. (1823). Mémoire sur les espèces du genre calmar (Loligo Lamarck). *Journal de Physique, de Chimie, d'Histoire naturelle et des Arts, 96*, 116-135. Retrieved from https://www.biodiversitylibrary.org/page/6176264

Bowen, G. J. (2010). Isoscapes: spatial pattern in isotopic biogeochemistry. *Annual Review of Earth and Planetary Sciences, 38*, 161-187.

Brodziak, J. K. T., & Macy, W. K. (1996). Growth of long-finned squid, *Loligo pealei*, in the northwest Atlantic. *Fishery Bulletin, 94*(2), 212-236.

Bullard, J. K. (2012). 2013 Atlantic mackerel, squid, and butterfish specifications and management measures: environmental assessment, regulatory impact review, initial regulatory flexibility analysis.

Buresch, K. C., Gerlach, G., & Hanlon, R. T. (2006). Multiple genetic stocks of longfin squid *Loligo pealeii* in the NW Atlantic: stocks segregate inshore in summer, but aggregate offshore in winter. *Marine Ecology Progress Series, 310*, 263-270. Retrieved from https://www.int-res.com/articles/meps2006/310/m310p263.pdf

Cadrin, S. X. (1998). *Status of fishery resources off the Northeastern United States for 1998* (S. Clark Ed. Vol. 115): US Department of Commerce, National Oceanic and Atmospheric Administration, National Marine Fisheries Service, Northeast Reigon Northeast Fisheries Science Center.

Carpenter, E. J., Harvey, H. R., Fry, B., & Capone, D. G. (1997). Biogeochemical tracers of the marine cyanobacterium Trichodesmium. *Deep Sea Research Part I: Oceanographic Research Papers, 44*(1), 27-38.

Carpenter, K. E. (2002). *The living marine resources of the Western Central Atlantic. Volume 1: Introduction, molluscs, crustaceans, hagfishes, sharks, batoid fishes and chimaeras*: FAO Library.

Ceriola, L., & Milone, N. (2007). Cephalopods age determination by statoliths reading: a technical manual. *AdriaMed Technical Documents*(22), 78 pp. Retrieved from http://www.faoadriamed.org/pdf/publications/web-td-22.pdf

Clarke, M. R. (1965). "Growth rings" in the beaks of the squid *Moroteuthis ingens* (Oegopsida: Onychoteuthidae). *Malacologia, 3*, 287-307.

Cohen, A. C. (1976). The systematics and distribution of Loligo (Cephalopoda, Myopsida) in the western North Atlantic, with descriptions of two new species. *Malacologia, 15*(2), 299-367.

Coplen, T. B., Brand, W. A., Gehre, M., Gröning, M., Meijer, H. A. J., Toman, B., & Verkouteren, R. M. (2006). New guidelines for δ 13C measurements. *Analytical Chemistry, 78*(7), 2439-2441.

Craig, S. (2001). *Environmental conditions and yolk biochemistry: factors influencing embryonic development in the squid Loligo forbesi (Cephalopoda: Loliginidae) Steenstrup 1856*: University of Aberdeen (United Kingdom).

Dawe, E. G., & Beck, P. C. (1997). Population structure, growth, and sexual maturation of short-finned squid (*Illex illecebrosus*) at Newfoundland. *Canadian Journal of Fisheries and Aquatic Sciences, 54*(1), 137-146.

DeNiro, M. J., & Epstein, S. (1978). Influence of diet on the distribution of carbon isotopes in animals. *Geochimica et cosmochimica acta, 42*(5), 495-506.

Forsythe, J. W. (2004). Accounting for the effect of temperature on squid growth in nature: from hypothesis to practice. *Marine and Freshwater Research, 55*(4), 331-339.

Fry, B. (1981). Natural stable carbon isotope tag traces Texas shrimp migrations. *Fishery Bulletin, 79*(2), 337-345.

González, A. F., Castro, B. G., & Guerra, A. (1996). Age and growth of the short-finned squid Illex coindetii in Galician waters (NW Spain) based on statolith analysis. *ICES Journal of Marine Science, 53*, 802-810.

Graham, B. S., Koch, P. L., Newsome, S. D., McMahon, K. W., & Aurioles, D. (2010). Using isoscapes to trace the movements and foraging behavior of top predators in oceanic ecosystems. *Isoscapes*, 299-318.

GSMFC. (2023). FIN Data Management System. Retrieved from https://www.gsmfc.org/fin-dms.php

Guarneros-Narváez, P. V., Rodríguez-Canul, R., De Silva-Dávila, R., Zamora-Briseño, J. A., Améndola-Pimenta, M., Souza, A. J., . . . Velázquez-Abunader, I. (2022). Loliginid paralarvae from the Southeastern Gulf of Mexico: Abundance, distribution, and genetic structure. *Frontiers in Marine Science, 9*, 941908.

Hatfield, E. M. C., & Cadrin, S. X. (2002). Geographic and temporal patterns in size and maturity of the longfin inshore squid (*Loligo pealeii*) off the northeastern United States. *Fishery Bulletin, 100*(2), 200-213.

Hatfield, E. M. C., Hanlon, R. T., Forsythe, J. W., & Grist, E. P. M. (2001). Laboratory testing of a growth hypothesis for juvenile squid Loligo pealeii (Cephalopoda: Loliginidae). *Canadian Journal of Fisheries and Aquatic Sciences, 58*(5), 845-857.

Herke, S. W., & Foltz, D. W. (2002). Phylogeography of two squid (*Loligo pealei* and *L. plei*) in the Gulf of Mexico and northwestern Atlantic Ocean. *Marine Biology, 140*(1), 103-115.

Hernández-Sánchez, O. G., Camacho-Ibar, V. F., Barbero, L., Herguera, J. C., & Herzka, S. Z. (2023). A gulf-wide synoptic isoscape of zooplankton isotope ratios reveals the importance of nitrogen fixation in supporting secondary production in the central Gulf of Mexico. *Frontiers in Marine Science*.

Hixon, R. F., Hanlon, R. T., Gillespie, S. M., & Griffin, W. L. (1980). Squid fishery in Texas: biological, economic, and market considerations. *Mar. Fish. Rev, 42*(7-8), 23-38.

Hobson, K. A. (1999). Tracing origins and migration of wildlife using stable isotopes: a review. *Oecologia, 120*(3), 314-326.

Hobson, K. A., & Cherel, Y. (2006). Isotopic reconstruction of marine food webs using cephalopod beaks: new insight from captively raised Sepia officinalis. *Canadian Journal of Zoology, 84*(5), 766-770.

Hunsicker, M. E., & Essington, T. E. (2008). Evaluating the potential for trophodynamic control of fish by the longfin inshore squid (*Loligo pealeii*) in the Northwest Atlantic Ocean. *Canadian Journal of Fisheries and Aquatic Sciences, 65*(11), 2524-2535.

Hunsicker, M. E., Essington, T. E., Aydin, K. Y., & Ishida, B. (2010). Predatory role of the commander squid *Berryteuthis magister* in the eastern Bering Sea: insights from stable isotopes and food habits. *Marine Ecology Progress Series, 415*, 91-108.

Jackson, G. D. (1994). Application and future potential of statolith increment analysis in squids and sepioids. *Canadian Journal of Fisheries and Aquatic Sciences, 51*(11), 2612-2625.

Jackson, G. D., Bustamante, P., Cherel, Y., Fulton, E. A., Grist, E. P. M., Jackson, C. H., . . . Ward, R. D. (2007). Applying new tools to cephalopod trophic dynamics and ecology: perspectives from the Southern Ocean Cephalopod Workshop, February 2–3, 2006. *Reviews in Fish Biology and Fisheries, 17*(2), 79-99.

Jacobson, L. D. (2005). Essential fish habitat source document. Longfin inshore squid, *Loligo pealeii*, life history and habitat characteristics.

Jacobson, L. D., Hendrickson, L. C., & Tang, J. (2015). Solar zenith angles for biological research and an expected catch model for diel vertical migration patterns that affect stock size estimates for longfin inshore squid (*Doryteuthis pealeii*). *Canadian Journal of Fisheries and Aquatic Sciences, 72*(9), 1329-1338.

Jereb, P., & Roper, C. F. E. (2010). *Cephalopods of the world. An annotated and illustrated catalogue of cephalopod species known to date. Volume 2. Myopsid and Oegopsid Squids*: FAO.

Kristensen, T. K. (1980). Periodical growth rings in cephalopod statoliths. *Dana, 1*, 39-51.

LaRoe, E. T. (1967). *A contribution to the biology of the Loliginidae (Cephalopoda: Myopsida) of the tropical western Atlantic.* (M.S.). University of Miami (unpublished),

Le-Alvarado, M., Romo-Curiel, A. E., Sosa-Nishizaki, O., Hernández-Sánchez, O., Barbero, L., & Herzka, S. Z. (2021). Yellowfin tuna (Thunnus albacares) foraging habitat and trophic position in the Gulf of Mexico based on intrinsic isotope tracers. *PloS one, 16*(2), e0246082.

Lesueur, C. A. (1821). Descriptions of several new species of cuttlefish. *Journal of the Academy of Natural Sciences of Philadelphia, 2*(1), 86-101.

Lipinski, M. R., Durholtz, M. D., & Underhill, L. G. (1998). Field validation of age readings from the statoliths of chokka squid (*Loligo vulgaris reynaudii* d'Orbigny, 1845) and an assessment of associated errors. *ICES Journal of Marine Science, 55*(2), 240-257.

Liu, B. L., Chen, X. J., Chen, Y., & Hu, G. Y. (2015). Determination of squid age using upper beak rostrum sections: technique improvement and comparison with the statolith. *Marine Biology, 162*(8), 1685-1693.

Liu, B. L., Xu, W., Chen, X. J., Huan, M. Y., & Liu, N. (2020). Ontogenetic shifts in trophic geography of jumbo squid, Dosidicus gigas, inferred from stable isotopes in eye lens. *Fisheries Research, 226*, 105507.

Locarnini, R. A., Mishonov, A. V., Baranova, O. K., Boyer, T. P., Zweng, M. M., Garcia, H. E., . . . Smolyar, I. V. (2019). World ocean atlas 2018, volume 1: Temperature. *NOAA Atlas NESDIS 81, 1*, 52.

Love, M. S., Baldera, A., Yeung, C., & Robbins, C. (2013). *The Gulf of Mexico ecosystem: A coastal & marine atlas*: Ocean Conservancy, Gulf Restoration Center.

Macy, W. K. (1995). The application of digital image processing to aging of long-finned squid, Loligo pealei, using the statolith. In (pp. 283-302): University of South Carolina Press.

Macy, W. K., & Brodziak, J. K. T. (2001). Seasonal maturity and size at age of *Loligo pealeii* in waters of southern New England. *ICES Journal of Marine Science, 58*, 852-864.

Madsen, P. T., Wilson, M., Johnson, M., Hanlon, R. T., Bocconcelli, A., De Soto, N. A., & Tyack, P. L. (2007). Clicking for calamari: toothed whales can echolocate squid *Loligo pealeii*. *Aquatic Biology, 1*(2), 141-150.

McCutchan Jr, J. H., Lewis Jr, W. M., Kendall, C., & McGrath, C. C. (2003). Variation in trophic shift for stable isotope ratios of carbon, nitrogen, and sulfur. *Oikos, 102*(2), 378-390.

McMahon, J. J., & Summers, W. C. (1971). Temperature effects on the developmental rate of squid (Loligo pealei) embryos. *The Biological Bulletin, 141*, 561-567.

McMahon, K. W., Hamady, L. L., & Thorrold, S. R. (2013). A review of ecogeochemistry approaches to estimating movements of marine animals. *Limnology and Oceanography, 58*(2), 697-714.

Meath, B. (2017). *Stable isotopes in the eye lenses of Doryteuthis plei: exploring natal origins and migratory patterns in the eastern Gulf of Mexico*: University of South Florida.

Meath, B., Peebles, E. B., Seibel, B. A., & Judkins, H. (2019). Stable isotopes in the eye lenses of *Doryteuthis plei* (Blainville 1823): Exploring natal origins and migratory patterns in the eastern Gulf of Mexico. *Continental Shelf Research, 174*, 76-84. doi:10.1016/j.csr.2018.12.013

Michaud, B. (2022). *Empirical and Modeled δ 13 C and δ 15 N Isoscapes in the Gulf of Mexico and Their Application to Fish Eye Lens Migration Studies.* University of South Florida,

Minagawa, M., & Wada, E. (1984). Stepwise enrichment of 15N along food chains: further evidence and the relation between δ15N and animal age. *Geochimica et cosmochimica acta, 48*(5), 1135-1140.

Montoya, J. P. (2007). Natural abundance of 15N in marine planktonic ecosystems. *Stable isotopes in ecology and environmental science*, 176-201.

Montoya, J. P., Carpenter, E. J., & Capone, D. G. (2002). Nitrogen fixation and nitrogen isotope abundances in zooplankton of the oligotrophic North Atlantic. *Limnology and Oceanography, 47*(6), 1617-1628.

Onthank, K. L. (2013). *Exploring the life histories of cephalopods using stable isotope analysis of an archival tissue*: Washington State University.

Parry, M. P. (2003). *The trophic ecology of two ommastrephid squid species, Ommastrephes bartramii and Sthenoteuthis oualaniensis, in the north Pacific sub-tropical gyre.* (PhD). University of Hawaii at Manoa,

Perez, J. A. A., O'Dor, R. K., Beck, P., & Dawe, E. G. (1996). Evaluation of gladius dorsal surface structure for age and growth studies of the short-finned squid, *Illex illecebrosus* (Teuthoidea: Ommastrephidae). *Canadian Journal of Fisheries and Aquatic Sciences, 53*(12), 2837-2846.

Peterson, B. J., & Fry, B. (1987). Stable isotopes in ecosystem studies. *Annual review of ecology and systematics, 18*(1), 293-320.

Qi, H., Coplen, T. B., Geilmann, H., Brand, W. A., & Böhlke, J. K. (2003). Two new organic reference materials for δ13C and δ15N measurements and a new value for the δ13C of NBS 22 oil. *Rapid Communications in Mass Spectrometry, 17*(22), 2483-2487.

Radabaugh, K. R., Hollander, D. J., & Peebles, E. B. (2013). Seasonal δ13C and δ15N isoscapes of fish populations along a continental shelf trophic gradient. *Continental Shelf Research, 68*, 112-122.

Radabaugh, K. R., & Peebles, E. B. (2014). Multiple regression models of δ13C and δ15N for fish populations in the eastern Gulf of Mexico. *Continental Shelf Research, 84*, 158-168. Retrieved from https://doi.org/10.1016/j.csr.2014.05.002

Radtke, R. L. (1983). Chemical and structural characteristics of statoliths from the short-finned squid *Illex illecebrosus*. *Marine Biology, 76*(1), 47-54.

Rosenberg, A. A., Wiborg, K. F., & Bech, I. M. (1981). Growth of Todarodes sagittatus (Lamarck)(Cephalopoda, Ommastrephidae) from the northeast Atlantic, based on counts of statolith growth rings. *Sarsia, 66*(1), 53-57.

SEAMAP Operations Manual for Trawl and Plankton Surveys. (2019). *Gulf States Marine Fisheries Commission*.

Serchuk, F. M., & Rathjen, W. F. (1974). Aspects of the distribution and abundance of the long-finned squid, *Loligo pealei*, between Cape Hatteras and Georges Bank. *Marine Fisheries Review, 36*(1), 10-17.

Sharp, Z. (2017). Principles of stable isotope geochemistry.

Shaw, P. W., Hendrickson, L., McKeown, N. J., Stonier, T., Naud, M. J., & Sauer, W. H. H. (2010). Discrete spawning aggregations of loliginid squid do not represent genetically distinct populations. *Marine Ecology Progress Series, 408*, 117-127.

Staudinger, M. D., & Juanes, F. (2010). A size-based approach to quantifying predation on longfin inshore squid *Loligo pealeii* in the northwest Atlantic. *Marine Ecology Progress Series, 399*, 225-241.

Stowasser, G., Pierce, G. J., Moffat, C. F., Collins, M. A., & Forsythe, J. W. (2006). Experimental study on the effect of diet on fatty acid and stable isotope profiles of the squid Lolliguncula brevis. *Journal of experimental marine biology and ecology, 333*(1), 97-114.

Summers, W. C. (1969). Winter population of Loligo pealei in the Mid-Atlantic Bight. *The Biological Bulletin, 137*, 202-216.

Vecchione, M. (1988). In-situ observations on a large squid-spawning bed in the eastern Gulf of Mexico. *Malacologia, 29*(1), 135-141.

Vecchione, M., Shea, E., Bussarawit, S., Anderson, F., Alexeyev, D., Lu, C. C., . . . Roper, C. (2005). Systematics of Indo-West Pacific loliginids. *Phuket Marine Biological Center Research Bulletin, 66*, 23-26.

Verrill, A. E. (1882). *Report on the cephalopods of the northeastern coast of America*: US Government Printing Office.
Voss, G. L. (1956). A review of the cephalopods of the Gulf of Mexico. *Bulletin of Marine Science of the Gulf and Caribbean, 6*(2), 85-178.
Wallace, A. A., Hollander, D. J., & Peebles, E. B. (2014). Stable isotopes in fish eye lenses as potential recorders of trophic and geographic history. *PloS one, 9*(10), e108935.
Werner, R. A., & Brand, W. A. (2001). Referencing strategies and techniques in stable isotope ratio analysis. *Rapid Communications in Mass Spectrometry, 15*(7), 501-519.
Werner, R. A., Bruch, B. A., & Brand, W. A. (1999). ConFlo III–an interface for high precision δ13C and δ15N analysis with an extended dynamic range. *Rapid Communications in Mass Spectrometry, 13*(13), 1237-1241.

APPENDICES

Appendix A. Linear regressions of $\delta^{13}C$ vs. diametric lamina midpoint for all specimens.

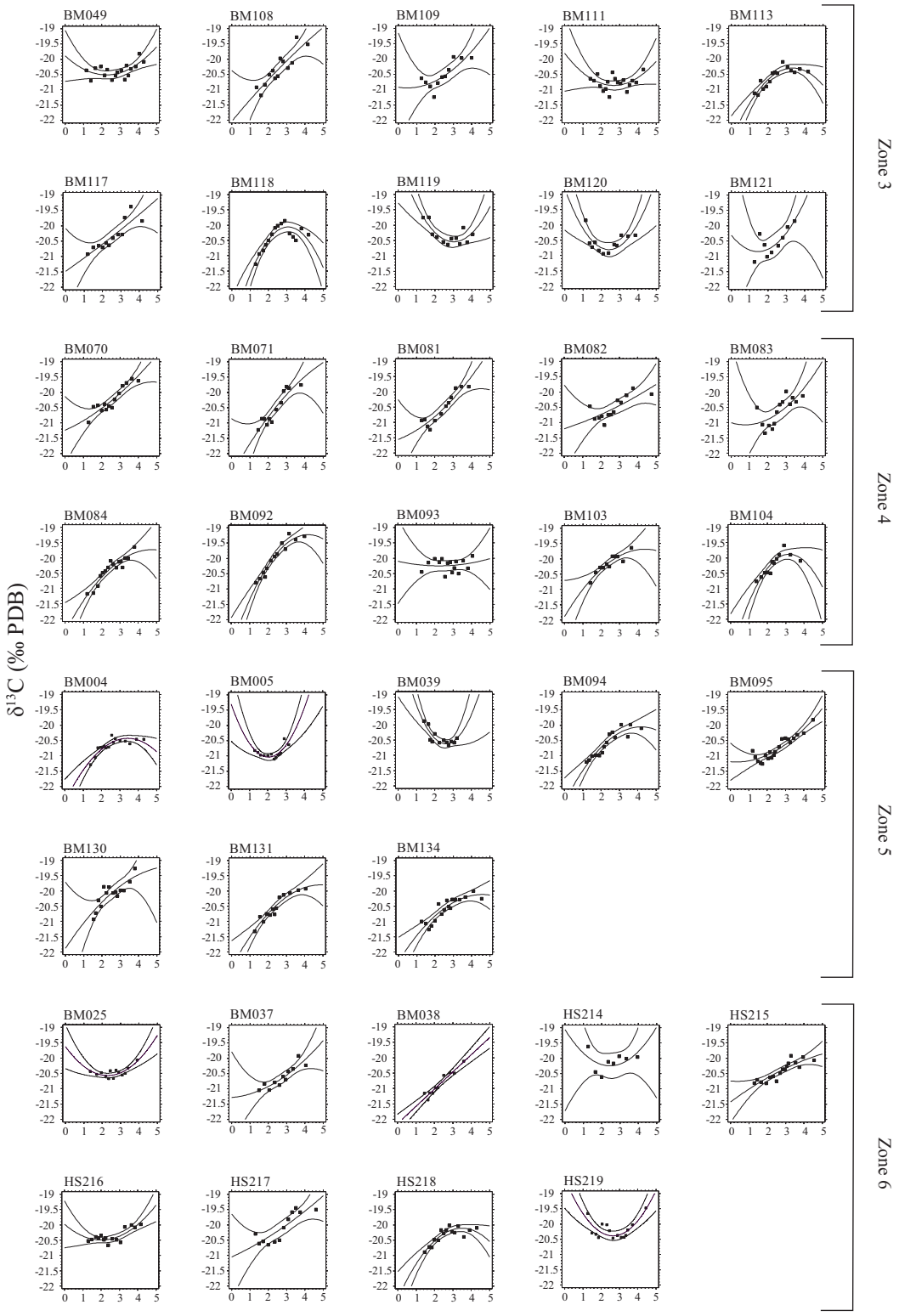

Appendix B. Linear regressions of $\delta^{15}N$ vs. diametric lamina midpoint for all specimens.

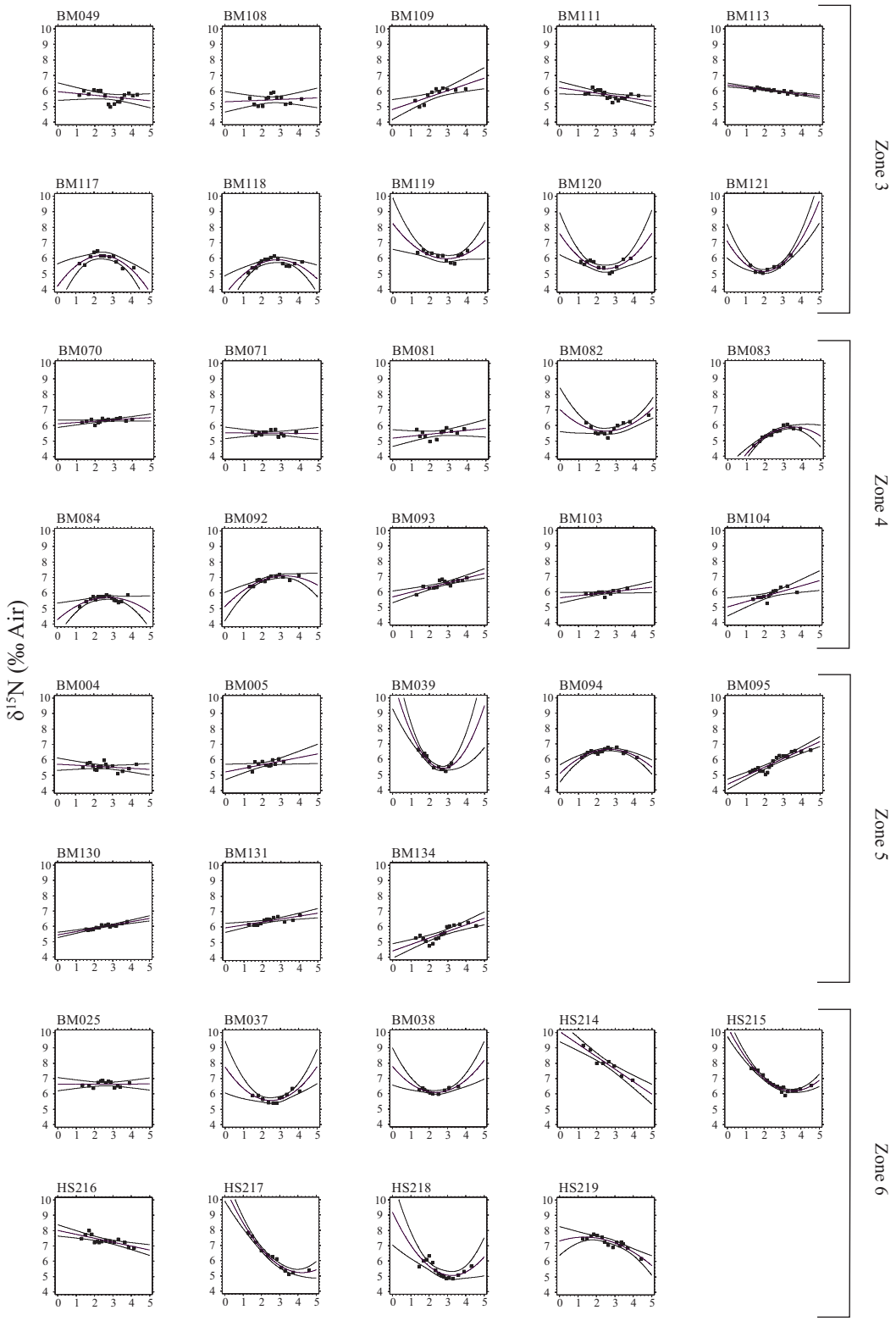

Appendix C. Spearman's rank correlations of $\delta^{15}N$ vs. $\delta^{13}C$ for all specimens.